

Bifurcations and multistability in a model of cytokine-mediated autoimmunity

Article (Accepted Version)

Fatehi, Farzad, Kyrychko, Yuliya N, Molchanov, Robert and Blyuss, Konstantin B (2019) Bifurcations and multistability in a model of cytokine-mediated autoimmunity. *International Journal of Bifurcation and Chaos*, 29 (3). 1950034 1. ISSN 0218-1274

This version is available from Sussex Research Online: <http://sro.sussex.ac.uk/id/eprint/79784/>

This document is made available in accordance with publisher policies and may differ from the published version or from the version of record. If you wish to cite this item you are advised to consult the publisher's version. Please see the URL above for details on accessing the published version.

Copyright and reuse:

Sussex Research Online is a digital repository of the research output of the University.

Copyright and all moral rights to the version of the paper presented here belong to the individual author(s) and/or other copyright owners. To the extent reasonable and practicable, the material made available in SRO has been checked for eligibility before being made available.

Copies of full text items generally can be reproduced, displayed or performed and given to third parties in any format or medium for personal research or study, educational, or not-for-profit purposes without prior permission or charge, provided that the authors, title and full bibliographic details are credited, a hyperlink and/or URL is given for the original metadata page and the content is not changed in any way.

Bifurcations and multi-stability in a model of cytokine-mediated autoimmunity

F. Fatehi¹, Y.N. Kyrychko¹, R. Molchanov², K.B. Blyuss^{1*}

¹ Department of Mathematics, University of Sussex, Falmer, Brighton BN1 9QH, UK

² Dnipropetrovsk Medical Academy of the Ministry of Health of Ukraine, Dnipro 49044, Ukraine

October 28, 2018

Abstract

This paper investigates the dynamics of immune response and autoimmunity with particular emphasis on the role of regulatory T cells (Tregs), T cells with different activation thresholds, and cytokines in mediating T cell activity. Analysis of the steady states yields parameter regions corresponding to regimes of normal clearance of viral infection, chronic infection, or autoimmune behaviour, and the boundaries of stability and bifurcations of relevant steady states are found in terms of system parameters. Numerical simulations are performed to illustrate different dynamical scenarios, and to identify basins of attraction of different steady states and periodic solutions, highlighting the important role played by the initial conditions in determining the outcome of immune interactions.

1 Introduction

Autoimmune disease is a pathological condition characterised by the failure of the immune system to efficiently discriminate between self-antigens and foreign antigens, resulting in unwanted destruction of healthy organ cells. In the case of normal functioning, recognition of foreign epitopes presented on antigen presenting cells (APCs) to T lymphocytes results in proliferation and effector function from T cells, while cross-reactivity between epitopes leads to the possibility of T cell response against self-antigens [1, 2]. T cells with high level of self-reactivity are removed from the system by two different mechanisms: central tolerance and peripheral tolerance. Central tolerance is associated with the removal of autoreactive T cells during their development in the thymus, while the peripheral tolerance is usually controlled by regulatory T cells [3]. One should note that it is important for autoreactive T cells to be present in the periphery to maintain effective T cell repertoire through generation of new peripheral T cells, and the stimulus produced by the healthy cells would normally not be sufficient to trigger activation of autoreactive T cells.

Clinical observations suggest that autoimmune disease is usually focused in a specific organ or part of the body, such as central nervous system in multiple sclerosis, retina in the case of uveitis, or pancreatic β -cells in insulin-dependent diabetes mellitus type-1 [4, 5, 6]. Significant efforts have

*Corresponding author: K.Blyuss@sussex.ac.uk

been made to pinpoint causes of autoimmune disease, and a large number of contributing factors have been identified, which include genetic predisposition, age, previous immune challenges, exposure to pathogens etc. [7]. One should note that even in the presence of genetic predisposition [8, 9, 10], further environmental triggers are required to initiate the onset of autoimmune disease, with infections being one of the main contributors [11, 12]. Spontaneous autoimmunity has been associated with the dysregulation of immune response against Epstein-Barr virus in patients with multiple sclerosis [13, 14, 15], while infections with Coxsackie viruses are associated with type-1 diabetes [16, 17]. A number of distinct mechanisms have been identified that explain how an infection of the host with a pathogen can subsequently trigger the onset of autoimmune disease. These mechanisms include bystander activation [18] and molecular mimicry [19, 16], which is particularly important in the context of autoimmunity caused by viral infections.

In terms of mathematical modelling of immune response and possible onset of autoimmunity, some of the early models analysed interactions between regulatory and effector T cells without investigating specific causes of autoimmunity, but instead focusing on T cell vaccination [20]. Borghans and De Boer [21] and Borghans *et al.* [22] showed how autoimmune dynamics, that they defined as above-threshold oscillations in the number of autoreactive cells, can appear in such models. Léon *et al.* [23, 24, 25] have studied interactions between different T cells, and how they can affect regulation of immune response and control of autoimmunity. Carneiro *et al.* [26] have presented an overview of that work and compared two possible mechanisms of immune self-tolerance that are either based on control by specific regulatory T cells, or result from tuning of T cell activation thresholds. Iawmi *et al.* [27, 28] have analysed a model of immune response to a viral infection with an emphasis on explicitly including the virus population, and the effects of different forms of the growth function for susceptible cells on autoimmune dynamics. Despite this model’s ability to demonstrate the emergence of autoimmunity, since it does not allow for a viral expansion, it cannot support a regime of normal viral clearance. Alexander and Wahl [29] have focused on how interactions of professional APCs with effector and regulatory T cells can control autoimmune response. Burroughs *et al.* [30, 31] have demonstrated how autoimmunity can arise through bystander activation mediated by cytokines. An excellent overview of some of the latest development in mathematical modelling of autoimmune disease can be found in a special issue on “Theories and modelling of autoimmunity” [32].

Since T cells are known to be fundamental for the dynamics of autoimmunity, several different methodologies have been proposed for the analysis of various roles they play in coordinating immune response. Experimental evidence suggests that a major component in controlling autoimmune behaviour is provided by regulatory T cells, which are activated by autoantigens and act to shut down immune responses [33, 34, 35], while impairment in the function of regulatory T cells results in autoimmune disease [36, 37]. To model this process, Alexander and Wahl [29] and Burroughs *et al.* [30, 31] have explicitly included a separate compartment for regulatory T cells that are activated by autoantigens and suppress the activity of autoreactive T cells. Another theoretical approach supported by experimental evidence is the idea that T cells have the capacity to adjust their activation threshold for response to stimulation by autoantigens depending on various environmental conditions or endogenous stochastic variation, which allows them to perform a variety of different immune functions. The associated framework of *tunable activation thresholds* was proposed for analysis of thymic [38] and peripheral T cell dynamics [39, 40], and has been subsequently used to analyse differences in activation/response thresholds that are dependent on the activation state of the T cell [41]. van den Berg and Rand [42] and Scherer *et al.* [43] have developed and analysed stochastic models for tuning of activation thresholds. The importance of tuning lies in the fact that it provides an effective mechanism for improving sensitivity and specificity of T cell signalling in a noisy environment [44, 45], and both murine and human experiments have confirmed that activation of T cells can indeed dynamically change during their circulation [46, 47, 48, 49]. It is noteworthy that the need for activation thresholds

for T cells can be derived directly from the first principles of signal detection theory [50].

To model the dynamics of immune response to a viral infection and possible onset of autoimmunity, Blyuss and Nicholson [51, 52] have proposed and analysed a mathematical model that includes two types of T cells with different activation thresholds and allows for a biologically realistic situation where infection and autoimmune response occur in different organs of the host. Depending on parameter values, this model can exhibit the regime of normal viral clearance, a chronic infection, and an autoimmune state represented by endogenous oscillations in cell populations, associated with episodes of high viral production followed by long periods of quiescence. Such behaviour, associated in the clinical practice with relapses and remissions, has been observed in a number of autoimmune diseases, such as MS, autoimmune thyroid disease, and uveitis [53, 54, 55]. Despite its successes, this model has several limitations. One of those is the fact that the periodic oscillations in the model are only possible when the amount of free virus and the number of infected cells are also exhibiting oscillations, while in laboratory and clinical situations, one rather observes a situation where autoimmunity follows full clearance of the initial infection. Another issue is that this model does not exhibit bi-stability, which could explain clinical observations suggesting that patients with very similar parameters of immune response can have significantly different course and outcome of the infection.

Bi-stability between different dynamical states is an extremely important property of various biological systems, and it has already been studied in a variety of contexts, including neural networks [56, 57, 58], gene regulatory networks [59, 60, 61], within-cell dynamics of RNA interference [62], and immune dynamics [63, 27]. In immunology, bifurcations and multi-stability have been studied in the context of T cell differentiation [64, 65], including the role of cytokines [66]. Ngina *et al.* [67] have investigated the dynamics of HIV from the perspective of interactions between HIV virions and CD8⁺ T cells, and identified a region of bi-stability associated with the backward bifurcation, where the system can reach either a virion-free or endemic equilibrium depending on the initial conditions. This observation has profound implications for developing an effective anti-retroviral therapy. Due to an important role played by immune response in mediating the onset and development of cancer, a number of researchers have investigated bifurcations and possible multi-stability that can arise in these interactions. Piotrowska [68] has analysed a model of immune response to malignant tumours with an emphasis on the role of time delay associated with developing immune response. This model was shown to exhibit bi-stability, with the dynamics being determined by the initial size of the tumour. Li and Levine [69] have investigated a cytokine-mediated bi-stability between immune-promoting and immune-suppressing states in the model of cancer-related inflammation. Anderson *et al.* [70] have looked into interactions between cytokines and CD4⁺ T cells for the purpose of immunotherapy. The bi-stability was shown to correspond to two simultaneously present levels at which the tumor can stabilise depending on the initial conditions.

In the specific context of autoimmunity, Léon *et al.* [23] have highlighted the importance of bi-stability between steady states with high populations of either regulatory, or effector T cells for effective representation of the adoptive transfer of tolerance. Roy *et al.* [71] have developed a general kinetic model to capture the role of vitamin D in immunomodulatory responses, and they demonstrated that vitamin D extends the region of bi-stability, thus allowing immune regulation to be more robust with respect to changes in pathogenic stimulation. Baker *et al.* [72] have analysed the dynamics of immune response during rheumatoid arthritis with particular emphasis on the effects of cytokines on bi-stability and treatment. Rapin *et al.* [73] have proposed a simple model of autoimmunity that displays a bi-stability between stable steady states corresponding to a healthy state and autoimmunity. The authors have shown how the system can be switched back to the healthy steady state by immunotherapy aimed at destabilising an autoimmune steady state.

In this paper, we will show how inclusion of regulatory T cells and the cytokine mediating T cell activity can allow one to overcome above-mentioned difficulties and provide a more realistic represen-

tation of various regimes in the dynamics of immune response. In the next section we will introduce the model and discuss its basic properties. Section 3 contains systematic analysis of all steady states, including conditions for their feasibility and stability. In Section 4 we perform extensive bifurcation analysis of the model and illustrate various types of behaviour that can be exhibited by the system depending on parameters and initial conditions, which includes identification of basins of attraction of various states. The paper concludes in Section 5 with the discussion of results.

2 Model derivation

To analyse the dynamics of immune response to infection and possible onset of autoimmunity, we use an approach similar to some of the earlier models of immune response [51, 52, 74, 75]. The underlying idea is the mechanism of molecular mimicry, where immune response against an infection can lead to a breakdown of immune tolerance due to cross-reaction with one or more self-antigens that share some of their immunological characteristics with a pathogen [16, 19]. Experimental evidence suggests that while antibodies are important in a wider picture of immune response to viral infections, within the context of autoimmunity, B cells can be dispensable, so that autoimmune disease can develop even in their absence [76]. Moreover, it has been shown in some studies that the development of antibodies can itself depend on prior interactions of T cells with a pathogen [77]. Hence, in this paper we rather focus on the role of T cells and associated cytokines.

We consider a situation where both infection and autoimmune response are targeting the same organ of the body, and the population of healthy cell in this organ is denoted by $A(t)$. These cells are assumed to follow logistic growth with the proliferation rate r and the carrying capacity N in the absence of infection or autoimmune response, as is common in models of viral dynamics [27, 78]. At the same time, one should be mindful of the fact that different functional forms of the growth of healthy cells can also have an effect on autoimmune dynamics, as has been shown by Iwami *et al.* [27, 28].

During a viral infection, some number of healthy cells become infected by free virus particles, at which point they move to the compartment of infected cells, denoted by $F(t)$. After a certain period of time, these infected cells will be producing virions, or free virus particles, $V(t)$ at a rate k , and the rate of natural clearance of virions is denoted by c . These virions then go on to infect other as yet uninfected cells at a rate β , which is an effective rate incorporating time constants associated with various biological processes, such as the movement of virions, cell entry, and an eclipse phase, during which the cells are infected but are not yet recognised as such by the immune system.

In terms of immune dynamics, T cell response originates in the lymph nodes. Stimulation of naïve T cells results in their proliferation, differentiation into activated T cells, and subsequent migration to the infected tissue. Once activated, T cells bearing the $CD8^+$ receptor become cytotoxic T cells that are able to destroy infected cells, whereas if they have a $CD4^+$ receptor, they turn into helper T cells [79, 80]. Tregs perform an important role of suppressing the autoreactive T cells, and are a part of $CD4^+$ T cell population [81, 82, 83]. Since in this paper we are trying to understand self and non-self discrimination mechanisms of the immune response, we consider two populations of naïve $CD8^+$ T cells that respond to self-antigens and foreign antigens, while focusing on one population of $CD4^+$ T cells representing regulatory T cells. Kim *et al.* [80] have considered a situation where each population of naïve T cells is maintained at a certain level supported by homeostasis in the absence of infection. Burroughs *et al.* [84, 30] and Segel *et al.* [20] in their models have instead considered a constant influx of new T cells from the thymus. In this model, for simplicity, we consider a single population of naïve T cells which includes Tregs, foreign-reactive and self-reactive T cells, and, similarly to earlier work, the population of these naïve T cells is assumed to be maintained at a certain level by homeostasis

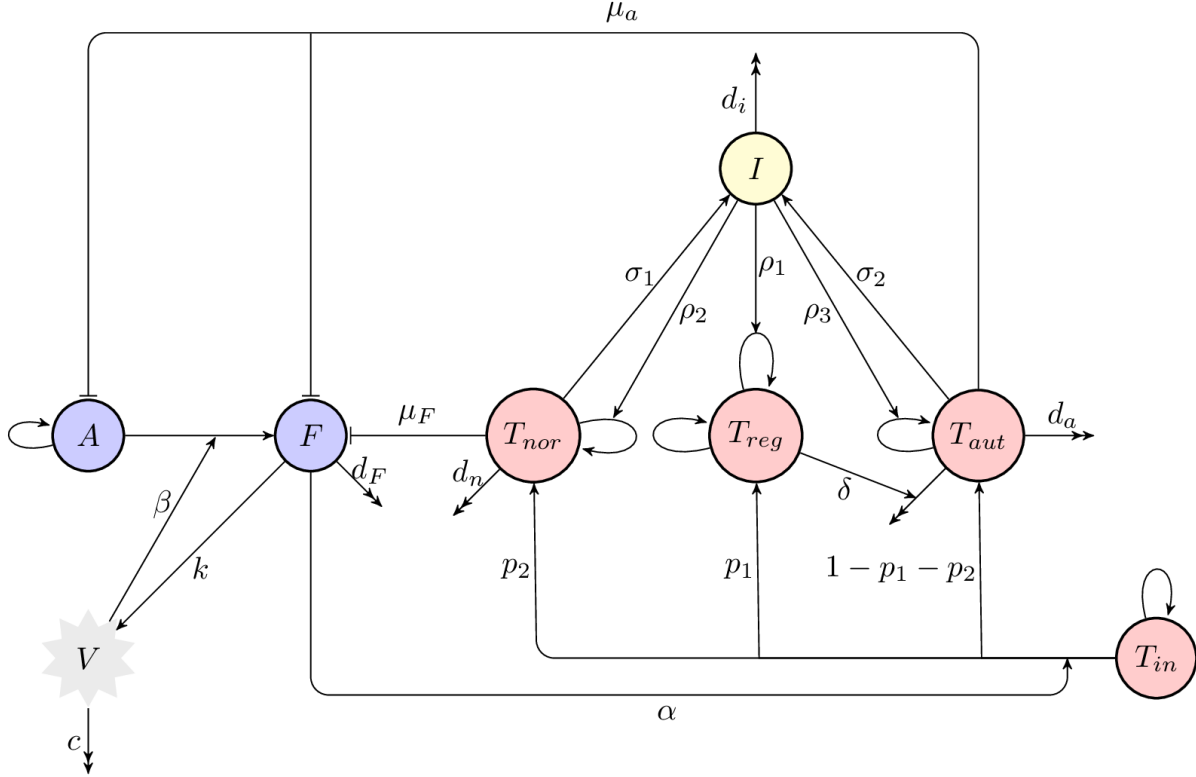


Figure 1: A schematic diagram of immune response to an infection. Blue circles indicate host cells (uninfected and infected cells), red circles denote different T cells (naïve, regulatory, normal activated, and autoreactive T cells), yellow circle shows cytokines (interleukin 2), and grey indicates virus particles (virions). Single arrow-headed and bar-headed lines indicate, respectively, production/proliferation and destroying of one cell population from/by another. Double arrows indicate natural clearance.

[51, 27, 28, 78]. It is thus assumed that in the absence of infection, these cells are produced at a constant rate λ_{in} , and they die at a rate d_{in} . Once activated, these cells differentiate into either regulatory T cells, whose main role is the control of immune response against self- and foreign antigens [79, 35], as well as prevention of autoimmune disease [35, 29, 26, 85], or effector cells that are able to eliminate infected cells. We denote by α the rate at which naïve T cells are activated. Since T_{in} includes different kinds of naïve T cells, it is assumed that a constant proportion p_1 of them will develop into regulatory T cells T_{reg} , and a proportion p_2 will become normal activated T cells T_{nor} that are able to recognise infected cells expressing foreign antigen and destroy these cells at rate μ_F . The remaining proportion $(1 - p_1 - p_2)$ of T cells will become autoreactive cells T_{aut} with a lower threshold for activation by healthy cells, hence, they will be destroying both infected and healthy cells at rate μ_a . Unlike the work by Blyuss and Nicholson [51, 52], Burroughs *et al.* [30] and Kim *et al.* [80] have not explicitly modelled the production of autoreactive T cells from normal activated T cells, and in the present model we also do not include this feature, as the model already accounts for the influx of each population of T cells directly to the tissue.

Similarly to other models of autoimmune dynamics [30, 84, 86], regulatory T cells in our model are assumed to have their own homeostatic mechanism, and they are assumed to be produced at constant rate λ_r and die at rate d_r . One of the main effects of regulatory T cells is to suppress the proliferation of autoreactive T cells. Part of this suppression occurs through the inhibition of interleukin 2 (IL-2) by T cells [87, 88]. Moreover, there is evidence for both cell-to-cell inhibition, and soluble mediators

such as IL-10 and TNF- β [84, 30, 33, 80]. There is some experimental evidence suggesting that the suppression by Tregs is antigen-specific [89, 90, 91], which implies that Tregs are able to discriminate between T cells responding to self-antigens and T cells responding to foreign antigen [35]. Léon *et al.* [23] and Carneiro *et al.* [92] have proposed a model that considers antigen-specific suppression by Tregs, thus endowing Tregs with a mechanism for self/non-self discrimination. Baecher-Allan *et al.* [93] have proposed a model for the T cell receptor (TCR) signal strength, where Tregs suppress the activation of autoreactive T cells, while the T cells reactive to foreign antigen are refractory to the suppression. Thus, in this paper we only consider direct suppression of autoreactive T cells by Tregs, which is assumed to occur at rate δ , and, unlike the work by Burroughs *et al.* [30] and Kim *et al.* [80], we are assuming Tregs do not suppress the normal activated T cells T_{nor} . Among various cytokines involved in the process of immune response, a particularly important role is played by IL-2, to be denoted by $I(t)$, which is an essential factor in the growth of T cells. Whilst this cytokine promotes the growth of both regulatory and effector T cells, regulatory T cells do not secrete IL-2 [79, 30, 84]. Therefore, in this model we assume that T_{nor} and T_{aut} produce IL-2 at rates σ_1 and σ_2 . On the other hand, whilst regulatory T cells do not produce IL-2, similar to other T cells they need this cytokine for their activation and proliferation [94, 95]. Thus, we assume that IL-2 promotes proliferation of T_{reg} , T_{nor} and T_{aut} at rates ρ_1 , ρ_2 and ρ_3 , respectively. Although it is also possible to include in the model inhibition of IL-2 by T cells [84, 95], our analysis shows that this would not qualitatively change the behaviour of the model.

With the above assumptions, the model for dynamics of immune response to a viral infection with account for Tregs, T cells with different activation thresholds and IL-2, as illustrated in Fig. 1, takes the form

$$\begin{aligned}
\frac{dA}{dt} &= rA \left(1 - \frac{A}{N}\right) - \beta AV - \mu_a T_{aut} A, \\
\frac{dF}{dt} &= \beta AV - d_F F - \mu_F T_{nor} F - \mu_a T_{aut} F, \\
\frac{dT_{in}}{dt} &= \lambda_{in} - d_{in} T_{in} - \alpha T_{in} F, \\
\frac{dT_{reg}}{dt} &= \lambda_r - d_r T_{reg} + p_1 \alpha T_{in} F + \rho_1 I T_{reg}, \\
\frac{dT_{nor}}{dt} &= p_2 \alpha T_{in} F - d_n T_{nor} + \rho_2 I T_{nor}, \\
\frac{dT_{aut}}{dt} &= (1 - p_1 - p_2) \alpha T_{in} F - d_a T_{aut} - \delta T_{reg} T_{aut} + \rho_3 I T_{aut}, \\
\frac{dI}{dt} &= \sigma_1 T_{nor} + \sigma_2 T_{aut} - d_i I, \\
\frac{dV}{dt} &= kF - cV,
\end{aligned} \tag{1}$$

with $0 \leq p_1 + p_2 \leq 1$. Introducing non-dimensional variables

$$\begin{aligned}
\hat{t} = rt, \quad A = N\hat{A}, \quad F = N\hat{F}, \quad T_{in} = \frac{\lambda_{in}}{d_{in}}\hat{T}_{in}, \quad T_{reg} = \frac{\lambda_{in}}{d_{in}}\hat{T}_{reg}, \\
T_{nor} = \frac{\lambda_{in}}{d_{in}}\hat{T}_{nor}, \quad T_{aut} = \frac{\lambda_{in}}{d_{in}}\hat{T}_{aut}, \quad I = \frac{\lambda_{in}}{d_{in}}\hat{I}, \quad V = N\hat{V},
\end{aligned}$$

yields a rescaled model

$$\begin{aligned}
\frac{dA}{dt} &= A(1 - A) - \beta AV - \mu_a T_{aut} A, \\
\frac{dF}{dt} &= \beta AV - d_F F - \mu_F T_{nor} F - \mu_a T_{aut} F, \\
\frac{dT_{in}}{dt} &= d_{in}(1 - T_{in}) - \alpha T_{in} F, \\
\frac{dT_{reg}}{dt} &= \lambda_r - d_r T_{reg} + p_1 \alpha T_{in} F + \rho_1 I T_{reg}, \\
\frac{dT_{nor}}{dt} &= p_2 \alpha T_{in} F - d_n T_{nor} + \rho_2 I T_{nor}, \\
\frac{dT_{aut}}{dt} &= (1 - p_1 - p_2) \alpha T_{in} F - d_a T_{aut} - \delta T_{reg} T_{aut} + \rho_3 I T_{aut}, \\
\frac{dI}{dt} &= \sigma_1 T_{nor} + \sigma_2 T_{aut} - d_i I, \\
\frac{dV}{dt} &= kF - cV,
\end{aligned} \tag{2}$$

where

$$\begin{aligned}
\hat{\beta} &= \frac{\beta N}{r}, \quad \hat{\mu}_a = \frac{\mu_a \lambda_{in}}{r d_{in}}, \quad \hat{d}_F = \frac{d_F}{r}, \quad \hat{\mu}_F = \frac{\mu_F \lambda_{in}}{r d_{in}}, \quad \hat{d}_{in} = \frac{d_{in}}{r}, \\
\hat{\alpha} &= \frac{\alpha N}{r}, \quad \hat{\lambda}_r = \frac{\lambda_r d_{in}}{\lambda_{in} r}, \quad \hat{d}_n = \frac{d_n}{r}, \quad \hat{d}_a = \frac{d_a}{r}, \quad \hat{\rho}_i = \frac{\rho_i \lambda_{in}}{r d_{in}}, \quad i = 1, 2, 3, \\
\hat{\delta} &= \frac{\delta \lambda_{in}}{r d_{in}}, \quad \hat{\sigma}_1 = \frac{\sigma_1}{r}, \quad \hat{\sigma}_2 = \frac{\sigma_2}{r}, \quad \hat{d}_i = \frac{d_i}{r}, \quad \hat{k} = \frac{k}{r}, \quad \hat{c} = \frac{c}{r}, \quad \hat{d}_r = \frac{d_r}{r},
\end{aligned}$$

and all hats in variables and parameters have been dropped for simplicity of notation. The model (2) is clearly well-posed, i.e. its solutions remain non-negative for $t \geq 0$ for any non-negative initial conditions.

3 Steady states and their stability

As a first step in the analysis of model (2), we look at its steady states

$$S^* = (A^*, F^*, T_{in}^*, T_{reg}^*, T_{nor}^*, T_{aut}^*, I^*, V^*),$$

that can be found by equating to zero the right-hand sides of equations (2) and solving the resulting system of algebraic equations. High dimensionality of the system (2) results in a large number of possible steady states, so we now systematically study all of them. First, we consider a situation where at a steady state, there is no free virus population, i.e. $V^* = 0$, which immediately implies $F^* = 0$ and $T_{in}^* = 1$. In this case there are four possible steady states depending on whether T_{nor}^* and T_{aut}^* are each equal to zero or being positive. If $T_{nor}^* = T_{aut}^* = 0$, there are two steady states

$$S_1^* = \left(0, 0, 1, \frac{\lambda_r}{d_r}, 0, 0, 0, 0\right), \quad S_2^* = \left(1, 0, 1, \frac{\lambda_r}{d_r}, 0, 0, 0, 0\right),$$

of which S_1^* is always unstable, and S_2^* is stable if $cd_F - k\beta > 0$, unstable if $cd_F - k\beta < 0$, and undergoes a steady-state bifurcation at $cd_F - k\beta = 0$. For $T_{nor}^* \neq 0$ and $T_{aut}^* = 0$, we again have two steady states

$$S_3^* = \left(0, 0, 1, \frac{\lambda_r \rho_2}{\rho_2 d_r - \rho_1 d_n}, \frac{d_i d_n}{\sigma_1 \rho_2}, 0, \frac{d_n}{\rho_2}, 0 \right),$$

$$S_4^* = \left(1, 0, 1, \frac{\lambda_r \rho_2}{\rho_2 d_r - \rho_1 d_n}, \frac{d_i d_n}{\sigma_1 \rho_2}, 0, \frac{d_n}{\rho_2}, 0 \right),$$

but they are both unstable for any values of parameters.

In the case when $T_{nor}^* = 0$ and $T_{aut}^* \neq 0$, we have steady states S_5^* and S_6^* ,

$$S_5^* = \left(0, 0, 1, T_{reg}^*, 0, \frac{d_i (d_a + \delta T_{reg}^*)}{\rho_3 \sigma_2}, \frac{d_a + \delta T_{reg}^*}{\rho_3}, 0 \right),$$

$$S_6^* = \left(1 - \frac{\mu_a d_i (d_a + \delta T_{reg}^*)}{\rho_3 \sigma_2}, 0, 1, T_{reg}^*, 0, \frac{d_i (d_a + \delta T_{reg}^*)}{\rho_3 \sigma_2}, \frac{d_a + \delta T_{reg}^*}{\rho_3}, 0 \right),$$

where

$$T_{reg}^* = \frac{d_r \rho_3 - \rho_1 d_a \pm \sqrt{(d_r \rho_3 - \rho_1 d_a)^2 - 4 \rho_1 \delta \lambda_r \rho_3}}{2 \rho_1 \delta}.$$

The steady state S_5^* (respectively, S_6^*) is stable if the following conditions hold

$$P < \frac{d_a + \delta T_{reg}^*}{\rho_3} < \frac{d_n}{\rho_2}, \quad \delta \rho_1 (T_{reg}^*)^2 > \lambda_r \rho_3,$$

$$\rho_3 \lambda_r^2 + \rho_3 d_i \lambda_r T_{reg}^* - \rho_3 d_i d_a (T_{reg}^*)^2 - \delta (\rho_1 d_a + \rho_3 d_i) (T_{reg}^*)^3 - \rho_1 \delta^2 (T_{reg}^*)^4 > 0,$$

where

$$P = \begin{cases} \frac{\sigma_2}{\mu_a d_i}, & \text{for } S_5^*, \\ \frac{\sigma_2 (\beta k - cd_F)}{\mu_a d_i (c + \beta k)}, & \text{for } S_6^*. \end{cases}$$

This steady state undergoes a steady-state bifurcation if

$$\frac{d_a + \delta T_{reg}^*}{\rho_3} = P, \quad \text{or} \quad \frac{d_a + \delta T_{reg}^*}{\rho_3} = \frac{d_n}{\rho_2}, \quad \text{or} \quad \delta \rho_1 (T_{reg}^*)^2 = \lambda_r \rho_3,$$

and a Hopf bifurcation if

$$P < \frac{d_a + \delta T_{reg}^*}{\rho_3} < \frac{d_n}{\rho_2}, \quad \delta \rho_1 (T_{reg}^*)^2 > \lambda_r \rho_3,$$

$$\rho_3 \lambda_r^2 + \rho_3 d_i \lambda_r T_{reg}^* - \rho_3 d_i d_a (T_{reg}^*)^2 - \delta (\rho_1 d_a + \rho_3 d_i) (T_{reg}^*)^3 - \rho_1 \delta^2 (T_{reg}^*)^4 = 0.$$

The steady state with $T_{nor}^* \neq 0$ and $T_{aut}^* \neq 0$ only exists for a particular combination of parameters, namely, when

$$\delta \rho_2^2 \lambda_r = (\rho_3 d_n - \rho_2 d_a)(\rho_2 d_r - \rho_1 d_n),$$

and is always unstable.

When $V^* \neq 0$, all other state variables are also non-zero. In this case, the steady state S_7^* has T_{nor}^* and T_{aut}^* satisfying the following system of equations

$$\begin{aligned} & \alpha c \mu_a \rho_2 \sigma_2 (\beta k + c) (T_{aut}^*)^2 T_{nor}^* + \alpha c \rho_2 (\beta k \mu_a \sigma_1 + c \mu_F \sigma_2 + c \mu_a \sigma_1) T_{aut}^* (T_{nor}^*)^2 \\ & - (\alpha \beta c k d_i d_n \mu_a + \beta^2 k^2 d_{in} \rho_2 \sigma_2 + \alpha \beta c k \rho_2 \sigma_2 - \alpha c^2 d_F \rho_2 \sigma_2 + \alpha c^2 d_i d_n \mu_a) T_{aut}^* \\ & T_{nor}^* + \alpha c d_i d_{in} \mu_a p_2 (\beta k + c) T_{aut}^* + \alpha c^2 \mu_F \rho_2 \sigma_1 (T_{nor}^*)^3 - (\beta^2 k^2 d_{in} \rho_2 \sigma_1 \\ & + \alpha \beta c k \rho_2 \sigma_1 - \alpha c^2 d_F \rho_2 \sigma_1 + \alpha c^2 d_i d_n \mu_F) (T_{nor}^*)^2 + d_i (\alpha c^2 d_{in} \mu_F p_2 \\ & + \beta^2 k^2 d_{in} d_n + \alpha \beta c k d_n - \alpha c^2 d_F d_n) T_{nor}^* - \alpha c d_i d_{in} p_2 (c d_F - k \beta) = 0, \end{aligned}$$

$$\begin{aligned} & p_2 \rho_1 \rho_3 \sigma_2^2 (T_{aut}^*)^3 + \sigma_2 (-\delta d_i p_1 \rho_2 + p_1 \rho_1 \rho_2 \sigma_2 + p_2 \rho_1 \rho_2 \sigma_2 + 2 p_2 \rho_1 \rho_3 \sigma_1 \\ & - \rho_1 \rho_2 \sigma_2) (T_{aut}^*)^2 T_{nor}^* - d_i p_2 \sigma_2 (d_a \rho_1 + d_r \rho_3) (T_{aut}^*)^2 + \sigma_1 (-\delta d_i p_1 \rho_2 \\ & + 2 p_1 \rho_1 \rho_2 \sigma_2 + 2 p_2 \rho_1 \rho_2 \sigma_2 + p_2 \rho_1 \rho_3 \sigma_1 - 2 \rho_1 \rho_2 \sigma_2) T_{aut}^* (T_{nor}^*)^2 + d_i (\delta d_i d_n p_1 \\ & - d_a p_2 \rho_1 \sigma_1 - d_n p_1 \rho_1 \sigma_2 - d_n p_2 \rho_1 \sigma_2 - d_r p_1 \rho_2 \sigma_2 - d_r p_2 \rho_2 \sigma_2 - d_r p_2 \rho_3 \sigma_1 \\ & + d_n \rho_1 \sigma_2 + d_r p_2 \sigma_2) T_{aut}^* T_{nor}^* + p_2 d_i^2 (\delta \lambda_r + d_a d_r) T_{aut}^* + (1 - p_1 - p_2) T_{nor}^* \\ & [-\rho_1 \rho_2 \sigma_1^2 (T_{nor}^*)^2 + d_i \sigma_1 (d_n \rho_1 + d_r \rho_2) T_{nor}^* - d_i^2 d_n d_r] = 0, \end{aligned}$$

with the rest of state variables being given by

$$\begin{aligned} I^* &= \frac{\sigma_1 T_{nor}^* + \sigma_2 T_{aut}^*}{d_i}, \quad A^* = \frac{c (d_F + \mu_F T_{nor}^* + \mu_a T_{aut}^*)}{k \beta}, \quad V^* = \frac{1 - A^* - \mu_a T_{aut}^*}{\beta}, \\ F^* &= \frac{c V^*}{k}, \quad T_{in}^* = \frac{d_{in}}{d_{in} + \alpha F^*}, \quad T_{reg}^* = \frac{\lambda_r + p_1 \alpha T_{in}^* F^*}{d_r - \rho_1 I^*}. \end{aligned}$$

It does not prove possible to analyse stability of this steady state analytically, hence, one has to resort to numerical calculations.

Remark. Inclusion of a term corresponding to production of autoreactive T cells directly from normal activated T cells in a manner similar to Blyuss and Nicholson [51, 52] would make the steady states S_3^* and S_4^* infeasible, while having no major effect on stability of other steady states. Hence, it suffices to consider the above model without explicitly modelling the transition from T_{nor} to T_{aut} .

4 Numerical stability analysis and simulations

To investigate various dynamical scenarios that can be exhibited by the model, we now perform a comprehensive numerical analysis of stability of different steady states and identify their possible bifurcations. Analytical results from the previous section suggest that the disease-free steady state S_2^* is stable when $k\beta < cd_F$, and unstable when $k\beta > cd_F$. As will be shown below, there are some major differences in dynamics between these two parameter combinations, hence, we will analyse them separately. Since there are significant differences in the reported values of many of the model parameters, and some of them have not yet been properly measures, we fix the baseline values as given in Table 1, and perform a sweep of parameter space to identify the effects of varying these parameters. Since prior to the start of infection, the numbers of infected cells, normal activated T cells, and the amount of IL-2 are all equal to zero, the initial condition for the model is taken to be

$$(A(0), F(0), T_{in}(0), T_{reg}(0), T_{nor}(0), T_{aut}(0), I(0), V(0)) = (0.9, 0, 0.8, 0.7, 0, 0, 0, 0.4), \quad (3)$$

which indicates the presence of some number of free virus particles. Here the initial values of $A(0)$ and $T_{in}(0)$ are chosen randomly, with the only requirement that they do not exceed unity, in light of

Parameter	Value	Definition
β	3	Infection rate
μ_a	20	The rate of killing of uninfected cells by autoreactive T cells
d_F	1.1	Natural death rate of infected cells
μ_F	6	The rate of killing of infected cells by the normal T cells
d_{in}	1	Growth rate of naïve T cells
α	0.4	Rate of activation of naïve T cells by infected cells
λ_r	3	Growth rate of regulatory T cells
d_r	0.4	Natural death rate of regulatory T cells
p_1	0.4	Rate of conversion of naïve T cells into regulatory T cells
p_2	0.4	Rate of conversion of naïve T cells into normal T cells
ρ_1	10	Proliferation rate of regulatory T cells by interleukin 2 (IL-2)
ρ_2	0.8	Proliferation rate of normal T cells by interleukin-2 (IL-2)
ρ_3	2	Proliferation rate of autoreactive T cells by interleukin 2 (IL-2)
d_n	1	Natural death rate of normal T cells
d_a	0.001	Natural death rate of autoreactive T cells
δ	0.002	Rate of clearance of autoreactive T cells by regulatory T cells
σ_1	0.15	Rate of production of interleukin-2 (IL-2) by normal T cells
σ_2	0.2	Rate of production of interleukin-2 (IL-2) by autoreactive T cells
d_i	0.6	Natural clearance rate of IL-2
k	2	Rate of production of free virus
c	6	Natural clearance rate of free virus

Table 1: Table of parameters

the fact that we are considering a non-dimensionalised model. For analysis of basins of attraction, the values of $T_{reg}(0)$ and $V(0)$ will be varied. Figure 2 illustrates how system dynamics is affected by the parameters. Since the condition $k\beta < cd_F$ holds, the disease-free steady state S_2^* is always stable. However, the system can also have two other biologically feasible steady states S_5^* and S_6^* , which only exist, provided regulatory T cells do not grow too rapidly and do not clear autoreactive T cells too quickly. In the case where autoreactive T cells are very effective in killing infected cells (i.e. for higher μ_a), or when they are producing IL-2 at a slow rate (smaller σ_2), only the steady state S_5^* is feasible, which has the zero population of host cells A , while the steady state S_6^* with $A > 0$ can only exist when μ_a is relatively low (or σ_2 is high), and S_5^* is unstable. Provided the steady states S_5^* and S_6^* are feasible, decreasing the growth rate λ_r of regulatory T cells results in a supercritical Hopf bifurcation, which gives rise to stable periodic solutions around these steady states. Since the steady state S_5^* is characterised by $A = 0$, both regimes where this steady state is stable, or unstable with oscillations around it, biologically correspond to a situation where the host cells are dead. On the other hand, a periodic solution around S_6^* corresponds to a proper autoimmune response, whereby the infection is cleared, but the immune system still exhibits endogenous oscillations, as illustrated in Fig. 4(a)-(b). At the intersection of the lines of Hopf bifurcation and the steady-state bifurcation, one has the fold-Hopf (also known as zero-Hopf or saddle-node Hopf) bifurcation [96]. Importantly, the steady states S_5^* and S_6^* can only exist if the rate ρ_3 at which IL-2 promotes proliferation of autoreactive T cells is sufficiently high, and this minimum value of the rate ρ_3 increases linearly with the rate ρ_1 at which IL-2 promotes proliferation of regulatory T cells. Once feasible, the steady states S_5^* and S_6^* are stable for smaller values of ρ_3 and then undergo Hopf bifurcation, when ρ_3 is sufficiently increased.

Since for all parameter combinations in Fig. 2 the steady state S_2^* is stable, this means that the

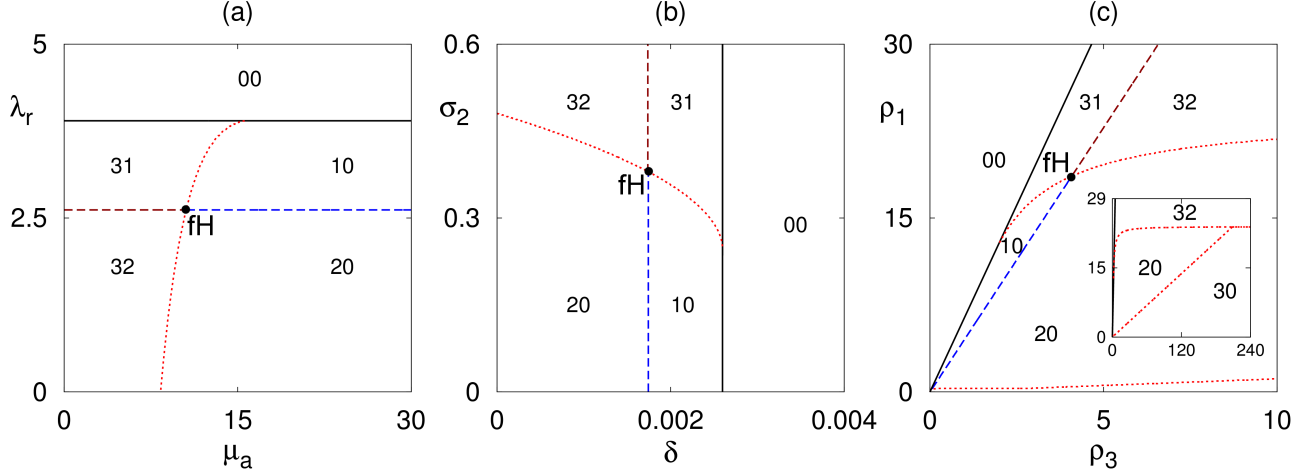


Figure 2: Regions of feasibility and stability of the steady states S_5^* and S_6^* with parameter values from Table 1. Black and red curves indicate the boundaries of feasibility and the steady-state bifurcation, whereas dashed lines (blue/brown) show the boundaries of Hopf bifurcation of the steady states S_5^* and S_6^* , respectively, with ‘fH’ indicating the fold-Hopf bifurcation. The first digit of the index refers to S_5^* , while the second corresponds to S_6^* , and they indicate that in that parameter region the respective steady state is unfeasible (index is ‘0’), stable (index is ‘1’), unstable via Hopf bifurcation with a periodic orbit around this steady state (index is ‘2’), or unstable via a steady-state bifurcation (index is ‘3’). In all plots, the condition $k\beta < cd_F$ holds, so the disease-free steady state S_2^* is also stable.

system can exhibit bi-stability between steady states and/or periodic solutions. To investigate this in more detail, we choose parameter values in the ‘32’ region in Fig. 2, where periodic oscillations around the steady state S_6^* are possible. While previous work on multi-stability in models of autoimmunity focussed mainly on identifying parameter regions associated with bi-stability [70, 72, 69], the structure of basins of attraction associated with different dynamical states has remained largely unexplored. To analyse basins of attraction in our model, due to high dimensionality of the phase space, we fix initial conditions for all state variables, and consider different initial amounts of free virus $V(0)$ and regulatory T cells $T_{reg}(0)$, as illustrated in Fig. 4. Biologically, this corresponds to varying the initial level of infection, as well as the initial state of the immune system, which can be primed by previous exposures to other pathogens. This Figure shows that if the initial number of regulatory T cells is sufficiently high, the system is able to successfully eliminate infection without any lasting consequences, settling on a stable disease-free steady state. Interestingly, for very small initial amounts of free virus, a higher amount of regulatory T cells is required to clear the infection. For lower values of $T_{reg}(0)$, the system exhibits stable periodic oscillations around the steady state S_6^* , which biologically represents the regime of autoimmune response. One can also observe that the minimum value of $T_{reg}(0)$ needed to achieve a disease-free steady state reduces with increasing the rate μ_F at which normal T cells are able to kill infected cells. Figure 4 illustrates temporary evolution of the system in the regime of bi-stability between a stable disease-free steady state and a periodic solution, corresponding to autoimmunity. The dynamics of regulatory T cells (not shown in this figure) mimics that of autoreactive T cells.

Next, we consider a situation described by the combination of parameters satisfying $k\beta > cd_F$, so the disease-free steady state S_2^* is unstable, and the system can only have steady states S_5^* , S_6^* , and S_7^* . Figure 5 shows how feasibility and stability of these steady states depend on parameters. Naturally, this figure is identical to Fig. 2 in terms of indicating stability and bifurcations of the steady states S_5^* and S_6^* . One should note that unlike the case considered earlier, now for sufficiently high rate σ_2 of production of IL-2, or sufficiently small rate μ_a at which autoreactive T cells are killing infected

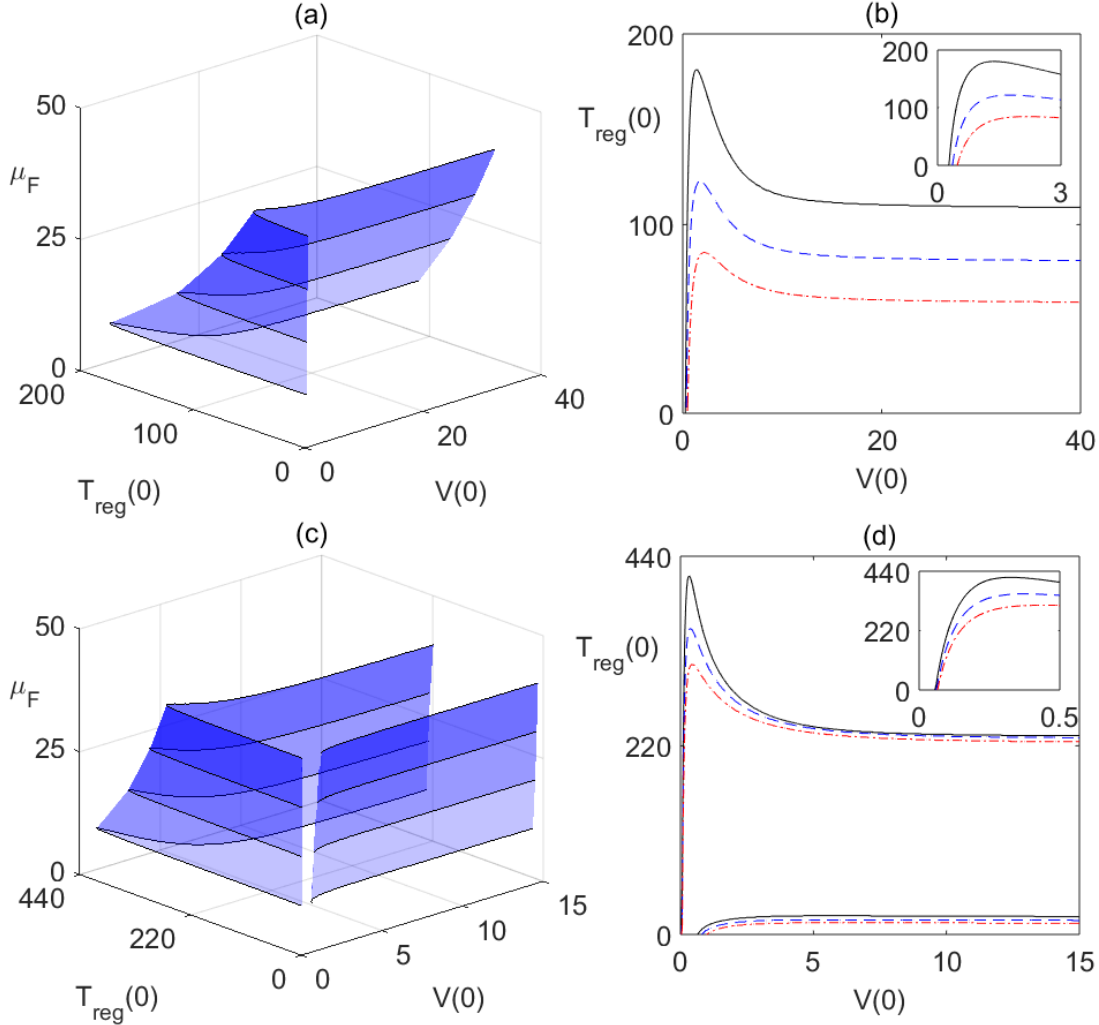


Figure 3: Regions of bi-stability with parameter values from Table 1 and initial condition (3). (a), (b) $\lambda_r = 2.5$, $\mu_a = 5$, with $\mu_F = 10$ (black), $\mu_F = 20$ (blue), $\mu_F = 30$ (red). The system exhibits autoimmune response to the right of the surface in (a) and below the curves in (b), while to the left of the surface in (a) and above the curves in (b) it tends to a stable disease-free steady state S_2^* . (c), (d) $\rho_1 = 30$, $\rho_3 = 8$. The system exhibits autoimmune response inside the region bounded by the surfaces in (c), or by the curves in (d), and outside it tends to a stable disease-free steady state S_2^* .

cells, the steady state S_6^* can also undergo a steady-state bifurcation due to the fact that the condition $k\beta > cd_F$ holds. Beyond this stability boundary, i.e. for very high values of σ_2 or very small values of μ_a , both steady states S_5^* and S_6^* are unstable, and the system settles either on the steady state S_7^* , or on a periodic solution around this steady state. In the parameter region, where only the steady state S_7^* is feasible, this steady state can only be unstable, giving rise to stable periodic oscillations, for sufficiently small values of δ or λ_r , whereas for higher values of those parameters this steady state is stable.

Figure 6 demonstrates the basins of attraction of the steady states S_5^* , S_6^* and S_7^* , as well as periodic solutions around them. As it has already been mentioned, this is the first time when basins of attraction for different steady states and periodic solutions are identified in a model of cytokine-mediated immune response and autoimmunity. Figure (a) shows that if the initial amount of free

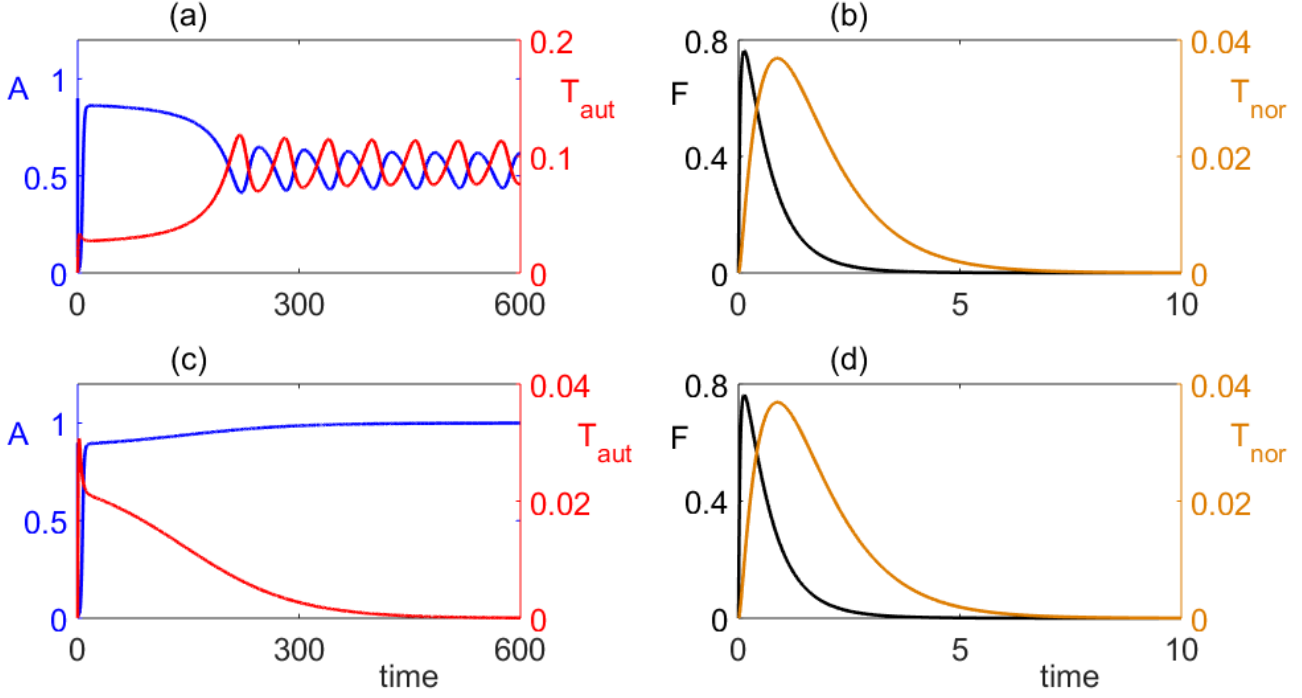


Figure 4: Simulation of the model (2) with parameter values from Table 1, except for $\lambda_r = 2.5$, $\mu_a = 5$, $\mu_F = 10$, and the initial condition (3). (a), (b) $V(0) = 10$, $T_{reg}(0) = 100$, the system exhibits periodic behaviour around S_6^* , i.e. clearance of infection followed by the onset of autoimmune response. (c), (d) $V(0) = 10$, $T_{reg}(0) = 150$, the model converges to a stable disease-free steady state S_2^* .

virus is sufficiently small, the system will converge to S_7^* for any value of $T_{reg}(0)$. For higher values of $V(0)$, the system exhibits bi-stability, where for smaller initial numbers of regulatory T cells $T_{reg}(0)$ it converges to the stable steady state S_5^* corresponding to the death of susceptible organ cells, while for higher values of $T_{reg}(0)$, the system settles on the stable steady state S_7^* . While the critical value of $T_{reg}(0)$ at which the transition between the two steady state takes place initially increases with $V(0)$, eventually it settles on some steady level, so that for higher initial amounts of free virus, this critical value no longer depends on $V(0)$. Figure (b) illustrates a qualitatively similar behaviour for higher rates of production of IL-2 and clearance of autoreactive T cells, in which case there is a bi-stability between S_6^* and S_7^* , but with the difference that there is also a small region for small values of $T_{reg}(0)$ and intermediate values of $V(0)$, where the system also converges to S_7^* . Figures (c) and (d) illustrate bi-stability between a periodic solution around S_7^* and either the stable steady state S_6^* , or a periodic solution around this steady state.

Numerical simulations in Figs. 7, 8, 9, and 10 show the dynamics of the model in the case when $k\beta > cd_F$ for the same parameter values but different initial conditions, thus illustrating various bi-stability scenarios shown in Fig. 6, in which crosses indicate the values of specific initial conditions used for simulations. Figure 7 demonstrates how for sufficiently small initial number of regulatory T cells the infection can result in the death of organ cells, in which case the system approaches a stable steady state S_5^* . On the other hand, for a higher number of Tregs, the system goes to a stable steady state S_7^* which represents a persistent (chronic) infection. In this case, one observes some kind of balance maintained with the help of regulatory T cells: while the immune system is not able to clear the infection, at the same time it prevents infection from destroying the organ cells.

Figure 8 illustrates a similar behaviour, where bi-stability takes place between the steady states S_6^* and S_7^* . In this case, for a smaller number of regulatory T cells, the system favours the regime

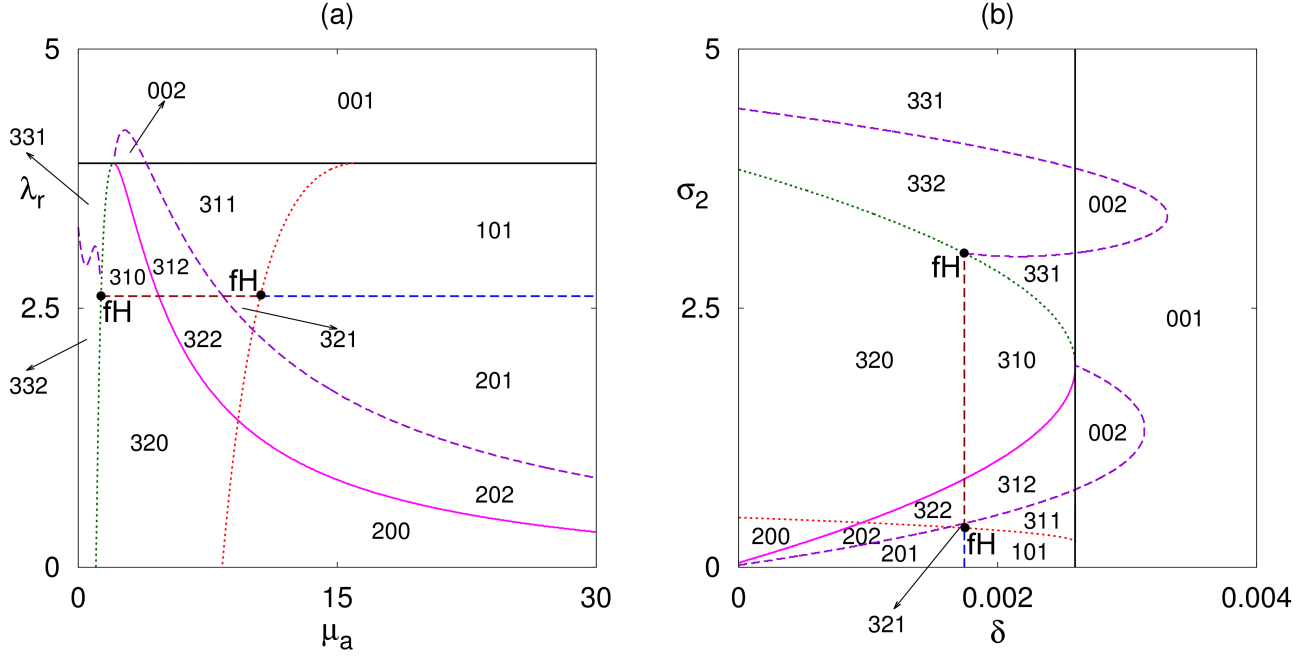


Figure 5: Regions of feasibility and stability of the steady states S_5^* , S_6^* , and S_7^* with parameter values from Table 1. Black and magenta curves indicates the boundaries of feasibility for S_5^*/S_6^* and S_7^* , dashed curves are the boundaries of Hopf bifurcation for S_5^*/S_6^* (blue/brown) or S_7^* (purple), and dotted lines are the boundaries of the steady-state bifurcation of S_5^* (red) and S_6^* (green), with ‘fH’ indicating the location of the fold-Hopf bifurcation. The first digit of the index refers to S_5^* , the second corresponds to S_6^* , and the third corresponds to S_7^* . These indices indicate that in that parameter region the respective steady state is unfeasible (index is ‘0’), stable (index is ‘1’), unstable via Hopf bifurcation with a periodic orbit around this steady state (index is ‘2’), or unstable via a steady-state bifurcation (index is ‘3’). In all plots, the condition $k\beta > cd_F$ holds, so the disease-free steady state S_2^* is unstable.

of normal clearance of infection, where after the initial growth, the numbers of infected cells and activated T cells responding to foreign antigen go to zero. For higher numbers of regulatory T cells, the system again approaches a stable steady state S_7^* describing a persistent infection. This is a really interesting and counter-intuitive result, which suggests that whilst regulatory T cells play a major role in reducing autoimmune response during normal disease clearance, when they are present in high numbers, they are actually promoting the persistence of infection.

Figure 9 illustrates a regime of bi-stability between periodic solutions around the steady states S_6^* and S_7^* . Similarly to the case of stable disease-free steady state considered earlier, the periodic solution around S_6^* biologically corresponds to the regime of autoimmune response, where upon clearance of the initial infection, the immune system maintains endogenous oscillations, in which the growth of autoreactive T cells results in the destruction of some healthy organ cells, after which the number of autoreactive T cells decreases, and the organ cells recover.

One should note that since these oscillations take place around the steady state S_6^* , the mean concentration of organ cells is much lower than what it was before the infection. In the case of periodic oscillations around the steady state S_7^* , initially one observes a similar behaviour in terms of rapid growth of infected cells, followed by an expansion in the population of activated T cells recognising foreign antigen, but after the number of infected cells decreases, rather than go to zero, it

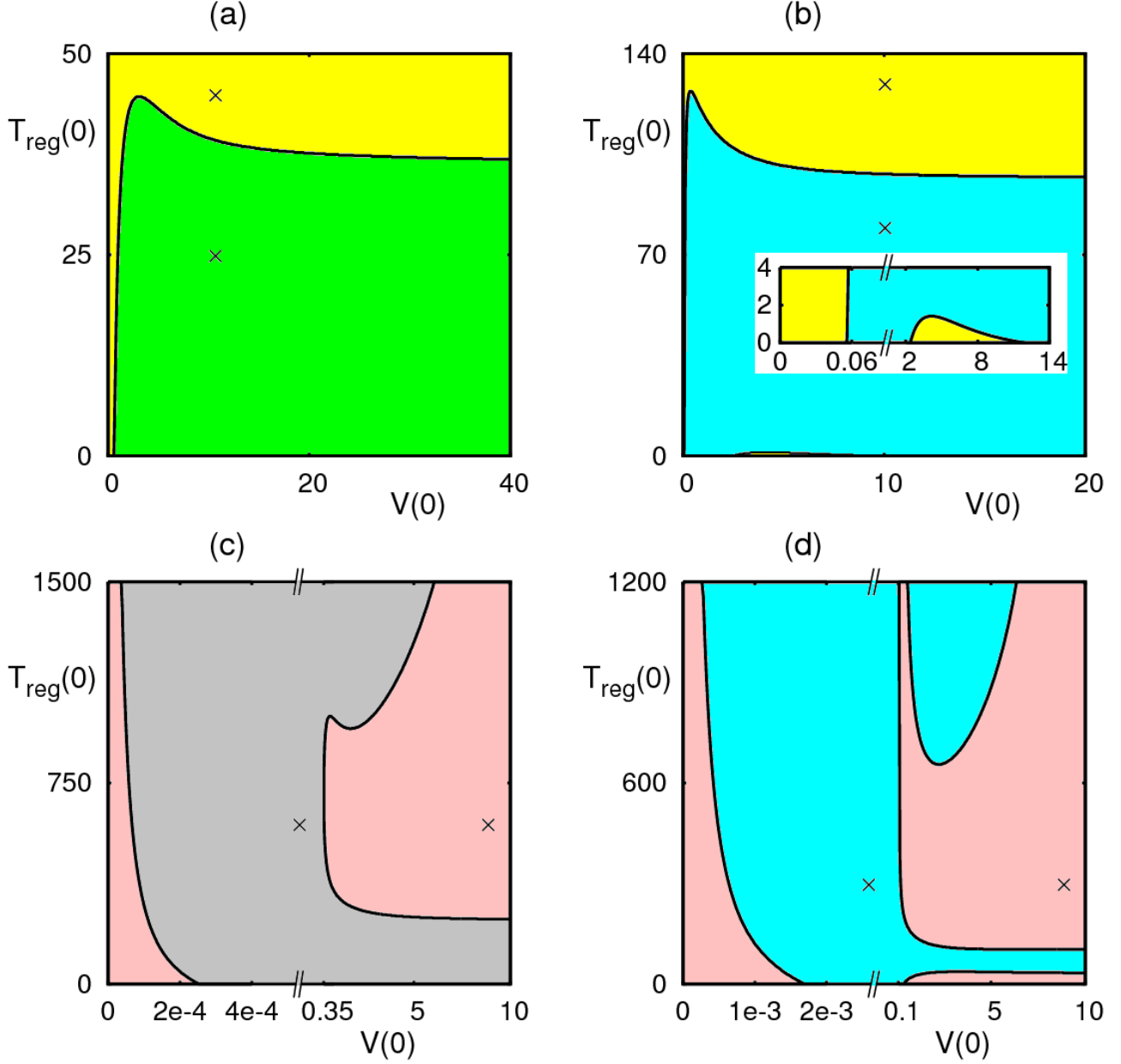


Figure 6: Regions of bi-stability in the system (2) with the initial condition (3), parameter values from Table 1, and $\beta = 4, k = 2.1$. (a) $\delta = 0.002, \sigma_2 = 0.2$, (b) $\delta = 0.0024, \sigma_2 = 0.5$, (c) $\delta = 0.0017, \sigma_2 = 0.42$, (d) $\delta = 0.0024, \sigma_2 = 0.7$. Green, blue and yellow are the basins of attraction of the steady states S_5^*, S_6^* , and S_7^* , respectively. Grey and pink are the basins of attraction of periodic solutions around S_6^* and S_7^* , respectively.

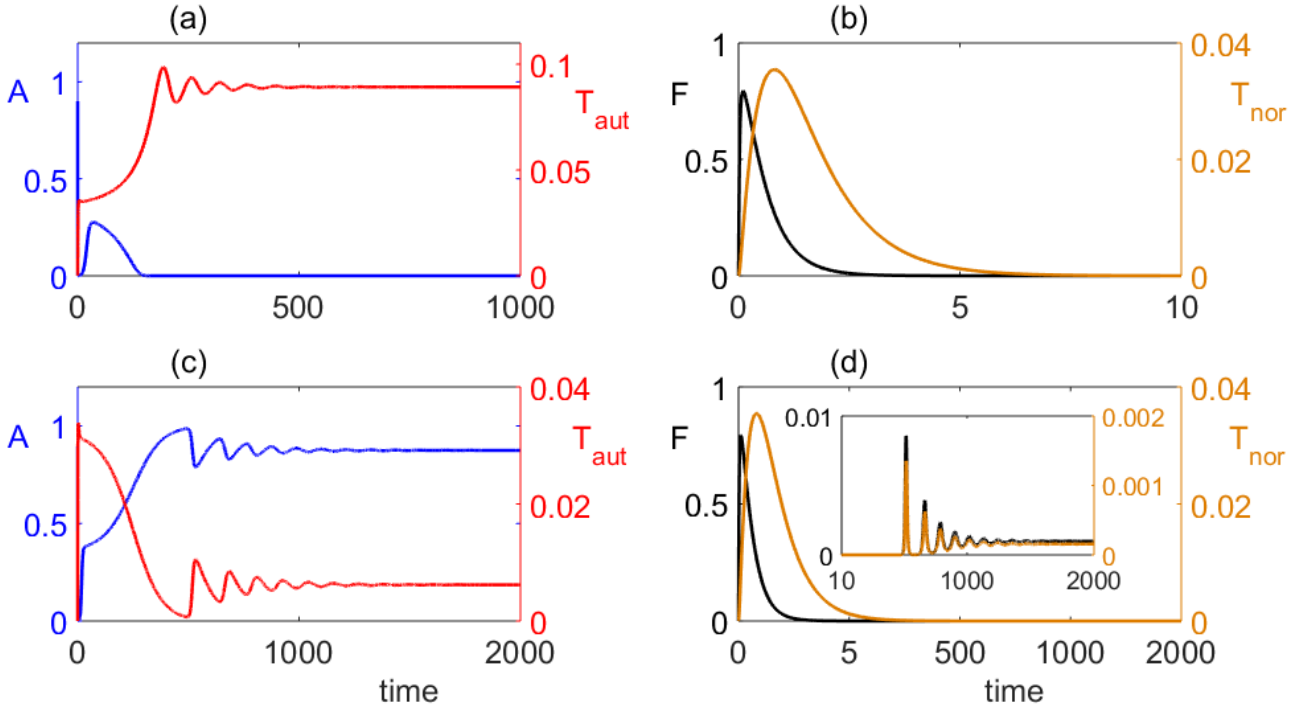


Figure 7: Numerical solution of the model (2) with the initial condition (3), parameter values from Table 1, and $\beta = 4$, $k = 2.1$, $\delta = 0.002$, $\sigma_2 = 0.2$. In (a) and (b) $V(0) = 10$ and $T_{reg}(0) = 25$. The model converges to the S_5^* . In (c) and (d) $V(0) = 10$ and $T_{reg}(0) = 45$. The model converges to the S_7^* . The dynamic of T_{reg} has a same behaviour as T_{aut} .

settles on periodic oscillations around some small positive level. This suggests that the infection is not cleared, but rather than being chronic, there are intervals of quiescence where the level of infection is very small, followed by regular intervals of rapid growth of infection and autoreactive T cells, which causes significant reduction in the number of uninfected organ cells. After this infection is significantly reduced by the activated T cells, the cycle repeats.

Finally, Figure 10 demonstrates a situation where the system has a bi-stability between a stable steady state S_6^* and a periodic solution around S_7^* . The difference from the previous case is that instead of autoimmune regime, the system can now successfully clear the infection, without having any subsequent oscillations. Although the infection itself is cleared, it leaves an imprint on the dynamics in the form of a reduced number of organ cells and a non-zero number of autoreactive T cells.

5 Discussion

In this paper we have developed and studied a model of immune response to a viral infection, with an emphasis on the role of cytokine mediating T cell activity, and T cells having different activation thresholds. Stability analysis of the model's steady states has allowed us to identify regimes with different dynamical behaviour depending on system parameters. When the product of infection rate and the rate of production of new virus particles is smaller than the product of the rates of viral clearance and death of infected cells, the immune system is able to successfully clear the infection without further consequences for either the host organ cells, or the immune system. In this case, the system settles on a stable disease-free steady state, characterised by the absence of infected cells and free virus, as well as zero amount of normal or autoreactive T cells. Another biologically feasible steady state that can exist in some parameter regimes is the state that also has no infected cells or

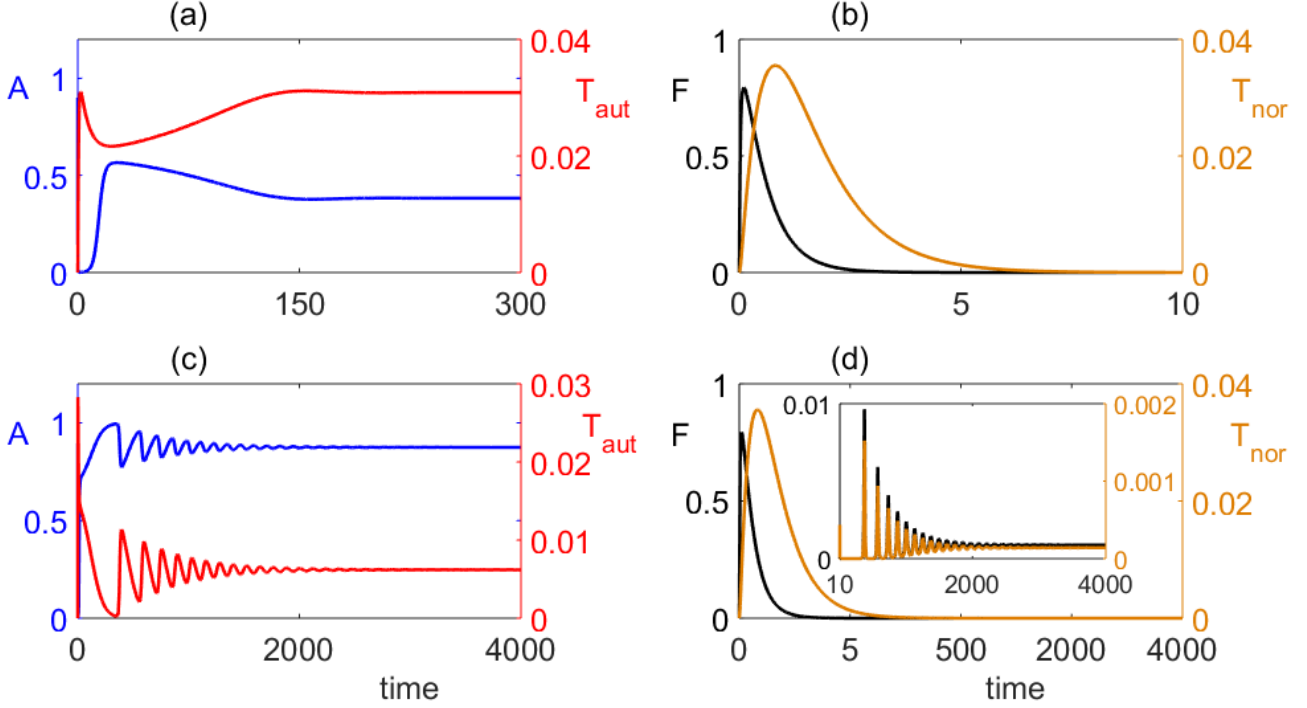


Figure 8: Numerical solution of the model (2) with the initial condition (3), parameter values from Table 1, and $\beta = 4$, $k = 2.1$, $\delta = 0.0024$, $\sigma_2 = 0.5$. (a), (b) $V(0) = 10$, $T_{reg}(0) = 80$. The system converges to S_6^* . (c), (d) $V(0) = 10$, $T_{reg}(0) = 130$. The system converges to S_7^* . The dynamics of T_{reg} is the same as T_{aut} .

free virus, but maintains non-zero levels of activated T cells. We have derived analytical conditions for steady-state and Hopf bifurcations of this state. When the disease-free steady state is unstable, the model also possesses a steady state with all cell populations being positive, which biologically corresponds to a state of chronic infection.

To investigate how the system behaves in different parameter regimes, we have solved it numerically, paying particular attention to cases where more than one steady state can be feasible. This has allowed us to identify regions of multi-stability, where for the same parameter values, depending on the initial conditions the system can approach either two distinct steady states, or a steady state and a periodic solution. In the case where the disease-free steady state is stable, such a regime has a very important potential clinical significance, as effectively it suggests that whether or not a given patient is able to clear the infection or will go on to develop autoimmunity depends not only on the rate of performance of their immune system, but also on the magnitude of viral challenge they experience and the amount of regulatory T cells they have before the infection. Numerical simulations for the autoimmune regime illustrate how initial infection leads to a rapid growth in the number of infected cells, resulting in the growth of populations of normal and autoreactive T cells, which clear the infection, but on a longer time-scale the system exhibits sustained periodic oscillations that can be associated with periods of relapses and remission, characteristic for many autoimmune diseases. For the case where the disease-free steady state is unstable, the bi-stability can occur between an autoimmune steady state and a chronic state, or a period orbit around the latter. A number of earlier models have looked into bi-stability in the immune dynamics, and the model analysed in this paper provides further clues regarding the important role played by cytokines in controlling the dynamics of immune response. In the regime of bi-stability, we have discovered that the initial state of the immune system, and the

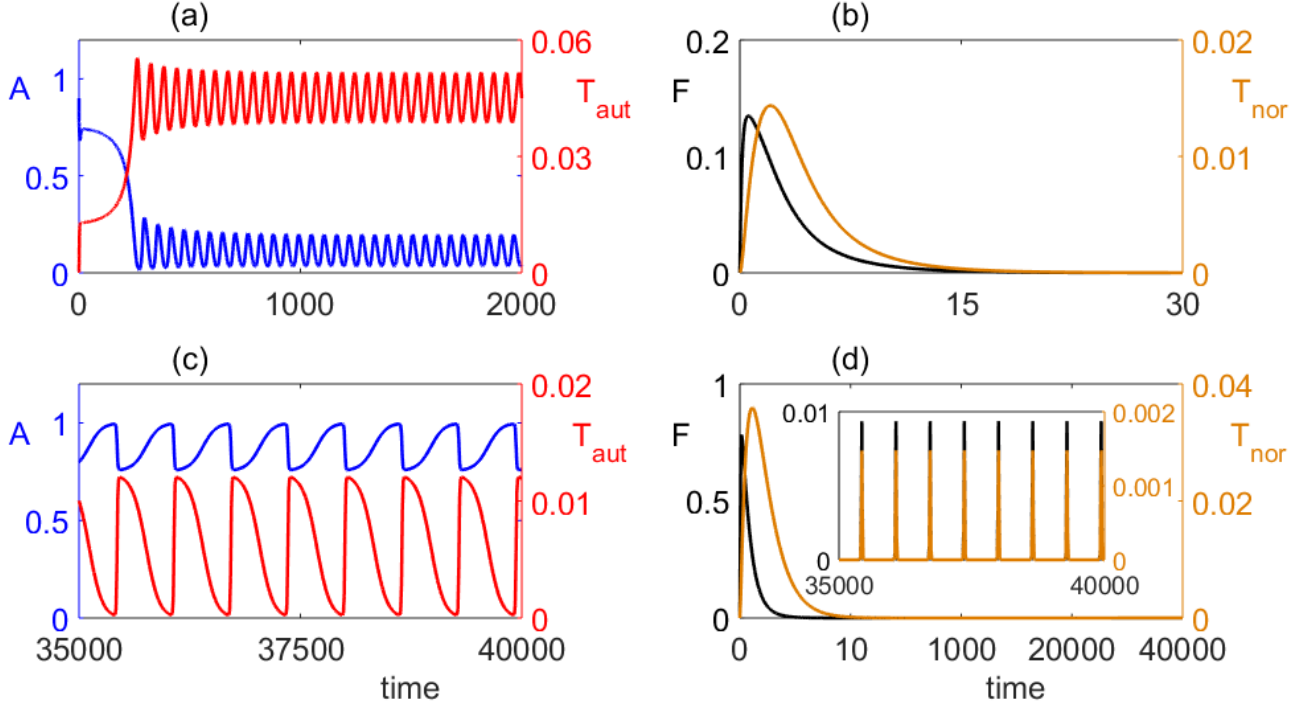


Figure 9: Numerical solution of the model (2) with the initial condition (3), parameter values from Table 1, and $\beta = 4$, $k = 2.1$, $\delta = 0.0017$, $\sigma_2 = 0.42$. (a), (b) $V(0) = 0.3$, $T_{reg}(0) = 600$. This system exhibits periodic oscillations around S_6^* , i.e. an autoimmune response. (c), (d) $V(0) = 9$, $T_{reg}(0) = 600$. The system exhibits periodic oscillations around S_7^* . The dynamics of T_{reg} is the same as T_{aut} .

initial viral load determine the course and outcome of the immune response, a result that would be interesting to test in an experimental setting.

There are several directions in which the model presented in this paper could be extended to make it more realistic. One possibility is to include in the model other potentially relevant aspects of immune system dynamics, such as memory T cells [97, 98], or the effects of T cells on secretion of IL-2 [84, 95]. Another aspect that is particularly relevant for our model is the fact that activation thresholds can themselves change during the process of immune response, hence, one could explicitly include the dynamics of activation thresholds as an extra component of the model [38, 41, 42, 43]. Many viruses are known to have a non-negligible lag phase in their virus cycle, which includes such processes as virus attachment, cell penetration and uncoating, virus assembly, maturation, and release of new virions. All these processes result in the delay in production and release of new virus particles, thus having an impact on the dynamics of immune response and potential onset and development of autoimmune disease. Mathematically, the lag phase can be represented using time delays in the relevant terms of the model, and the available data on lag phase for viruses associated with triggering or exacerbating autoimmune diseases can be used to validate the model.

Due to the large dimension of the phase space of model (2), and the complex structure of basins of attraction for different steady states and periodic solutions illustrated above, it would be important to more systematically investigate the issue of multi-stability in the system. One very promising approach to address this challenging problem is that of *offset boosting* [99, 100, 101, 102]. The underlying idea is that provided the model has the property that ensures that the functional form of equations remains the same when one of the state variables is shifted by a constant, this would imply that the system

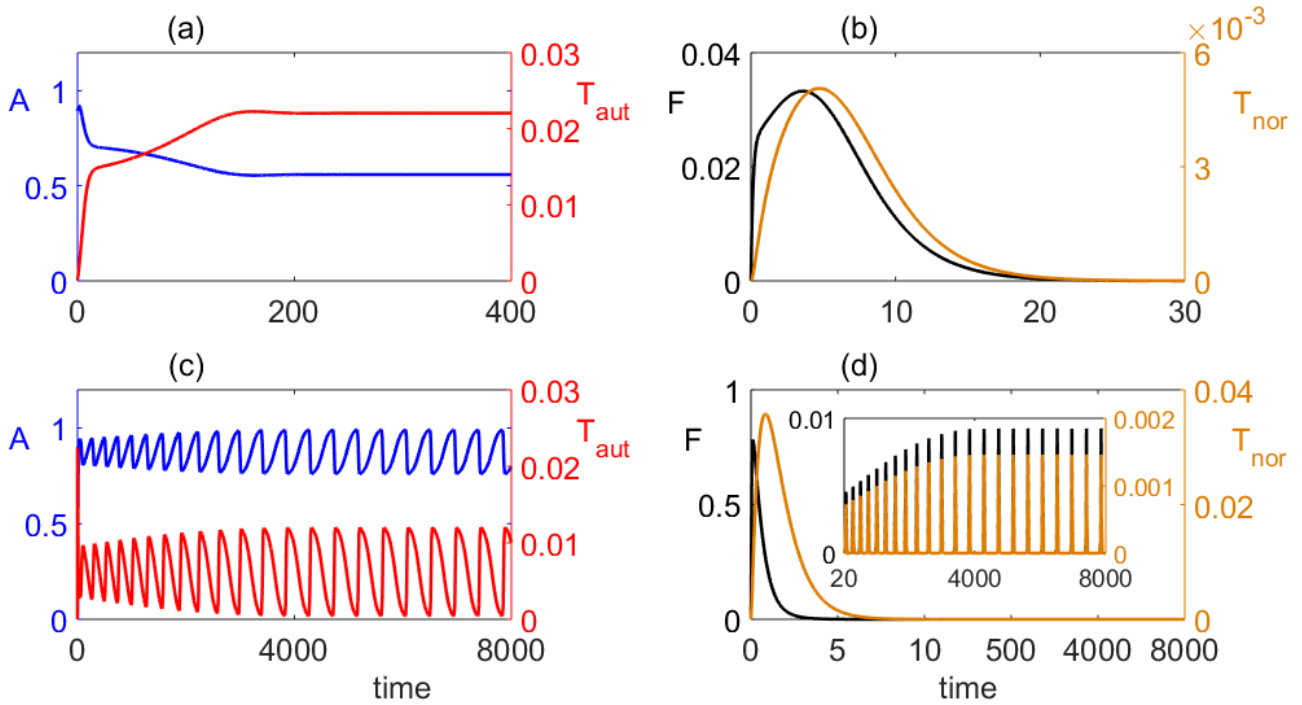


Figure 10: Numerical simulation of the model (2) with the initial condition (3), parameter values from Table 1, and $\beta = 4$, $k = 2.1$, $\delta = 0.0024$, $\sigma_2 = 0.7$. (a), (b) $V(0) = 0.05$, $T_{reg}(0) = 300$. The system converges to S_6^* . (c), (d) $V(0) = 9$, $T_{reg}(0) = 300$. The system exhibits periodic oscillations around S_7^* . The dynamics of T_{reg} is the same as T_{aut} .

is *variable-boostable*, and it can then be transformed into a system with *conditional symmetry* [102], implying that the new system is symmetric subject to a certain condition on the boosting. The importance of this conditional symmetry is two-fold. On the one hand, it provides a robust handle on identification of symmetric attractors in the system [102], which otherwise may not be apparent, especially due to a large dimensionality of the phase space. On the other hand, this methodology yields an effective tool for identifying multi-stability and exploring basins of attraction for different dynamical states, by allowing the system to visit different basins of attraction with the same initial condition by means of offset boosting [101]. Future work will explore model (2) from the perspective of conditional symmetry to identify all parameter regions associated with multi-stability and to delineate associated basins of attraction. This will provide significant practical insights for monitoring of onset and progress of autoimmune disease.

Acknowledgments

FF acknowledges the support from Chancellor's Studentship from the University of Sussex.

References

- [1] D. Mason, "A very high level of crossreactivity is an essential feature of the T-cell receptor," *Immunol. Today*, vol. 19, no. 9, pp. 395–404, 1998.

- [2] A. C. Anderson, H. P. Waldner, V. Turchin, C. Jabs, M. Prabhu Das, V. K. Kuchroo, and L. B. Nicholson, "Autoantigen responsive T cell clones demonstrate unfocused TCR cross-reactivity towards multiple related ligands: implications for autoimmunity," *Cell. Immunol.*, vol. 202, no. 2, pp. 88–96, 2000.
- [3] K. Wing, Z. Fehervari, and S. Sakaguchi, "Emerging possibilities in the development and function of regulatory T cells," *Int. Immunol.*, vol. 18, no. 7, pp. 991–1000, 2006.
- [4] E. C. Kerr, D. A. Copland, A. D. Dick, and L. B. Nicholson, "The dynamics of leukocyte infiltration in experimental autoimmune uveoretinitis," *Eye Res.*, vol. 27, no. 5, pp. 527–535, 2008.
- [5] E. Prat and R. Martin, "The immunopathogenesis of multiple sclerosis," *J. Rehabil. Res. Dev.*, vol. 39, no. 2, pp. 187–200, 2002.
- [6] P. Santamaria, "The long and winding road to understanding and conquering type 1 diabetes," *Immunity*, vol. 32, no. 4, pp. 437–445, 2010.
- [7] R. Root-Bernstein and D. Fairweather, "Unresolved issues in theories of autoimmune disease using myocarditis as a framework," *J. Theor. Biol.*, vol. 375, pp. 101–123, 2015.
- [8] A. L. Caforio and S. Illiceto, "Genetically determined myocarditis: clinical presentation and immunological characteristics," *Curr. Opin. Cardiol.*, vol. 23, no. 3, pp. 219–226, 2008.
- [9] H. S. Li, D. L. Ligon, and N. R. Rose, "Genetic complexity of autoimmune myocarditis," *Autoimmun. Rev.*, vol. 7, no. 3, pp. 168–173, 2008.
- [10] L. Guilherme, K. F. Kohler, E. Postol, and J. Kalil, "Genes, autoimmunity and pathogenesis of rheumatic heart disease," *Ann. Pediatr. Cardiol.*, vol. 4, no. 1, pp. 13–21, 2011.
- [11] D. Germolic, D. H. Kono, J. C. Pfau, and K. M. Pollard, "Animal models used to examine the role of environment in the development of autoimmune disease: findings from an NIEHS Expert Panel Workshop," *J. Autoimmun.*, vol. 39, no. 4, pp. 285–293, 2012.
- [12] M. P. Mallampalli, E. Davies, D. Wood, H. Robertson, F. Polato, and C. L. Carter, "Role of environmental and sex differences in the development of autoimmune disease: around table meeting report," *J. Womens Health*, vol. 22, no. 7, pp. 578–586, 2013.
- [13] J. Correale, M. Fiol, and W. Gilmore, "The risk of relapses in multiple sclerosis during systemic infections," *Neurology*, vol. 67, no. 4, pp. 652–659, 2006.
- [14] C. Münz, J. D. Lünemann, M. T. Getts, and S. D. Miller, "Antiviral immune responses: triggers of or triggered by autoimmunity?," *Nat. Rev. Immunol.*, vol. 9, no. 4, pp. 246–258, 2009.
- [15] A. Davidson and B. Diamond, "Autoimmune diseases," *N. Engl. J. Med.*, vol. 345, pp. 340–350., 2001.
- [16] A. M. Ercolini and S. D. Miller, "The role of infections in autoimmune disease," *Clin. Exp. Immunol.*, vol. 155, no. 1, pp. 1–15, 2009.
- [17] M. S. Horwitz, L. M. Bradley, J. Harbetson, T. Krah, J. Lee, and N. Sarvetnick, "Diabetes induced by Coxsackie virus: initiation by bystander damage and not molecular mimicry," *Nat. Med.*, vol. 4, no. 7, pp. 781–786, 1998.

- [18] R. S. Fujinami, “Can virus infections trigger autoimmune disease?,” *J. Autoimmun.*, vol. 16, no. 3, pp. 229–234, 2001.
- [19] M. G. von Herrath and M. B. A. Oldstone, “Virus-induced autoimmune disease,” *Curr. Opin. Immunol.*, vol. 8, no. 6, pp. 878–885, 1996.
- [20] L. A. Segel, E. Jäger, D. Elias, and I. R. Cohen, “A quantitative model of autoimmune disease and T-cell vaccination: does more mean less?,” *Immunol. Today*, vol. 16, no. 2, pp. 80–84, 1995.
- [21] J. A. M. Borghans and R. J. De Boer, “A minimal model for T-cell vaccination,” *Proc. R. Soc. Lond. B Biol. Sci.*, vol. 259, no. 1355, pp. 173–178, 1995.
- [22] J. A. M. Borghans, R. J. De Boer, E. Sercarz, and V. Kumar, “T cell vaccination in experimental autoimmune encephalomyelitis: a mathematical model,” *J. Immunol.*, vol. 161, no. 3, pp. 1087–1093, 1998.
- [23] K. León, R. Perez, A. Lage, and J. Carneiro, “Modelling T-cell-mediated suppression dependent on interactions in multicellular conjugates,” *J. Theor. Biol.*, vol. 207, no. 2, pp. 231–254, 2000.
- [24] K. León, A. Lage, and J. Carneiro, “Tolerance and immunity in a mathematical model of T-cell mediated suppression,” *J. Theor. Biol.*, vol. 225, no. 1, pp. 107–126, 2003.
- [25] K. León, J. Faro, A. Lage, and J. Carneiro, “Inverse correlation between the incidences of autoimmune disease and infection predicted by a model of T cell mediated tolerance,” *J. Autoimmun.*, vol. 22, no. 1, pp. 31–42, 2004.
- [26] J. Carneiro, T. Paixão, D. Milutinovic, J. Sousa, K. León, R. Gardner, and J. Faro, “Immunological self-tolerance: Lessons from mathematical modeling,” *J. Comput. Appl. Math.*, vol. 184, no. 1, pp. 77–100, 2005.
- [27] S. Iwami, Y. Takeuchi, Y. Miura, T. Sasaki, and T. Kajiwara, “Dynamical properties of autoimmune disease models: tolerance, flare-up, dormancy,” *J. Theor. Biol.*, vol. 246, no. 4, pp. 646–659, 2007.
- [28] S. Iwami, Y. Takeuchi, K. Iwamoto, Y. Naruo, and M. Yasukawa, “A mathematical design of vector vaccine against autoimmune disease,” *J. Theor. Biol.*, vol. 256, no. 3, pp. 382–392, 2009.
- [29] H. K. Alexander and L. M. Wahl, “Self-tolerance and autoimmunity in a regulatory T cell model,” *Bull. Math. Biol.*, vol. 73, no. 1, pp. 33–71, 2011.
- [30] N. J. Burroughs, M. Ferreira, B. M. P. M. Oliveira, and A. A. Pinto, “Autoimmunity arising from bystander proliferation of T cells in an immune response model,” *Math. Comput. Model.*, vol. 53, no. 7, pp. 1389–1393, 2011.
- [31] N. J. Burroughs, M. Ferreira, B. M. P. M. Oliveira, and A. A. Pinto, “A transcritical bifurcation in an immune response model,” *J. Diff. Eqns. Appl.*, vol. 17, pp. 1101–1106, 2011.
- [32] R. Root-Bernstein, “Theories and modeling of autoimmunity,” *J. Theor. Biol.*, vol. 375, pp. 1–124, 2015.
- [33] S. Sakaguchi, “Naturally arising $CD4^+$ regulatory T cells for immunologic self-tolerance and negative control of immune responses,” *Ann. Rev. Immunol.*, vol. 22, pp. 531–562, 2004.

- [34] S. Z. Josefowicz, L. F. Lu, and A. Y. Rudensky, “Regulatory T cells: mechanisms of differentiation and function,” *Ann. Rev. Immunol.*, vol. 30, pp. 531–564, 2012.
- [35] A. Corthay, “How do regulatory T cells work?,” *Scand. J. Immunol.*, vol. 70, no. 4, pp. 326–336, 2009.
- [36] J. D. Fontenot, M. A. Gavin, and A. Y. Rudensky, “Foxp3 programs the development and function of CD4⁺CD25⁺ regulatory T cells,” *Nat. Immunol.*, vol. 4, no. 4, pp. 330–336, 2003.
- [37] R. Khattri, T. Cox, S.-A. Yasayko, and F. Ramsdell, “An essential role for scurf in CD4⁺CD25⁺ T regulatory cells,” *Nat. Immunol.*, vol. 4, no. 4, pp. 337–342, 2003.
- [38] Z. Grossman and A. Singer, “Tuning of activation thresholds explains flexibility in the selection and development of T cells in the thymus,” *Proc. Natl. Acad. Sci. USA*, vol. 93, no. 25, pp. 14747–14752, 1996.
- [39] Z. Grossman and W. E. Paul, “Adaptive cellular interactions in the immune system: the tunable activation threshold and the significance of subthreshold responses,” *Proc. Natl. Acad. Sci. USA*, vol. 89, no. 21, pp. 10365–10369, 1992.
- [40] Z. Grossman and W. E. Paul, “Self-tolerance: context dependent tuning of T cell antigen recognition,” *Semin. Immunol.*, vol. 12, no. 3, pp. 197–203, 2000.
- [41] G. Altan-Bonnet and R. N. Germain, “Modeling T cell antigen discrimination based on feedback control of digital ERK responses,” *PLoS Biol.*, vol. 3, p. e356, 2005.
- [42] H. A. van den Berg and D. A. Rand, “Dynamics of T cell activation threshold tuning,” *J. Theor. Biol.*, vol. 228, no. 3, pp. 397–416, 2004.
- [43] A. Scherer, A. Noest, and R. J. de Boer, “Activation-threshold tuning in an affinity model for the T-cell repertoire,” *Proc. R. Soc. Lond. B Biol. Sci.*, vol. 271, no. 1539, pp. 609–616, 2004.
- [44] O. Feinerman, R. N. Germain, and G. Altan-Bonnet, “Quantitative challenges in understanding ligand discrimination by $\alpha\beta$ T cells,” *Mol. Immunol.*, vol. 45, no. 3, pp. 619–631, 2008.
- [45] A. J. T. George, J. Stark, and C. Chan, “Understanding specificity and sensitivity of T-cell recognition,” *Trends Immunol.*, vol. 26, no. 12, pp. 653–659, 2005.
- [46] A. D. Bitmansour, D. C. Douek, V. C. Maino, and L. J. Picker, “Direct ex vivo analysis of human CD4⁺ memory T cell activation requirements at the single clonotype level,” *J. Immunol.*, vol. 169, no. 3, pp. 1207–1218, 2002.
- [47] L. B. Nicholson, A. C. Anderson, and V. K. Kuchroo, “Tuning T cell activation threshold and effector function with cross-reactive peptide ligands,” *Int. Immunol.*, vol. 12, no. 2, pp. 205–213, 2000.
- [48] P. S. Römer, S. Berr, E. Avota, S.-Y. Na, M. Battaglia, I. ten Berge, H. Einsele, and T. Hünig, “Preculture of PBMC at high cell density increases sensitivity of T-cell responses, revealing cytokine release by CD28 superagonist TGN1412,” *Blood*, vol. 118, no. 26, pp. 6772–6782, 2011.
- [49] I. Stefanová, J. R. Dorfman, and R. N. Germain, “Self-recognition promotes the foreign antigen sensitivity of naive T lymphocytes,” *Nature*, vol. 420, no. 6914, pp. 429–434, 2002.

- [50] A. J. Noest, “Designing lymphocyte functional structure for optimal signal detection: *voilà*, T cells,” *J. Theor. Biol.*, vol. 207, pp. 195–216, 2000.
- [51] K. B. Blyuss and L. B. Nicholson, “The role of tunable activation thresholds in the dynamics of autoimmunity,” *J. Theor. Biol.*, vol. 308, pp. 45–55, 2012.
- [52] K. B. Blyuss and L. B. Nicholson, “Understanding the roles of activation threshold and infections in the dynamics of autoimmune disease,” *J. Theor. Biol.*, vol. 375, pp. 13–20, 2015.
- [53] D. Ben Ezra and J. V. Forrester, “Fundal white dots: the spectrum of a similar pathological process,” *Brit. J. Ophthalmol.*, vol. 79, no. 9, pp. 856–860, 1995.
- [54] T. F. Davies, D. C. Evered, B. Rees Smith, P. P. B. Yeo, F. Clark, and R. Hall, “Value of thyroid-stimulating-antibody determination in predicting the short-term thyrotoxic relapse in Graves’ disease,” *Lancet*, vol. 309, no. 8023, pp. 1181–1182, 1997.
- [55] A. Nylander and D. A. Hafler, “Multiple sclerosis,” *J. Clin. Invest.*, vol. 122, no. 4, pp. 1180–1188, 2012.
- [56] G. Bao and Z. Zeng, “Analysis and design of associative memories based on recurrent neural network with discontinuous activation functions,” *Neurocomp.*, vol. 77, pp. 101–107, 2012.
- [57] Q. Lai, B. Hu, Z.-H. Guan, T. Li, D.-F. Zheng, and Y.-H. Wu, “Multistability and bifurcation in a delayed neural network,” *Neurocomputing*, vol. 207, pp. 785–792, 2016.
- [58] L. Olien and J. Bélair, “Bifurcations, stability, and monotonicity properties of a delayed neural network model,” *Phys. D*, vol. 102, pp. 349–363, 1997.
- [59] S. Huang, G. Eichler, Y. Bar-Yam, and D. Ingber, “Cell fates as high-dimensional attractor states of a complex gene regulatory network,” *Phys. Rev. Lett.*, vol. 94, p. 128701, 2005.
- [60] Q. Lai, “Stability and bifurcation of delayed bidirectional gene regulatory networks with negative feedback loops,” *Chin. J. Phys.*, vol. 56, no. 3, pp. 1064–1073, 2018.
- [61] B. D. MacArthur, A. Ma’ayan, and I. R. Lemischka, “Systems biology of stem cell fate and cellular reprogramming,” *Nat. Rev. Mol. Cell Biol.*, vol. 10, pp. 672–681, 2009.
- [62] G. Neofytou, Y. N. Kyrychko, and K. B. Blyuss, “Time-delayed model of RNA interference,” *Ecol. Compl.*, vol. 30, pp. 11–25, 2017.
- [63] K. B. Blyuss and S. Gupta, “Stability and bifurcations in a model of antigenic variation in malaria,” *J. Math. Biol.*, vol. 58, pp. 923–937, 2009.
- [64] A. Yates, C. Bergmann, J. L. Van Hemmen, J. Stark, and R. Callard, “Cytokine-modulated regulation of helper T cell populations,” *J. Theor. Biol.*, vol. 206, pp. 539–560, 2000.
- [65] A. Leber, V. Abedi, R. Hontecillas, M. Viladomiu, S. Hoops, S. Ciupe, J. Caughman, T. Andrew, and J. Bassaganya-Riera, “Bistability analyses of CD4+ T follicular helper and regulatory cells during *Helicobacter pylori* infection,” *J. Theor. Biol.*, vol. 398, pp. 74–84, 2016.
- [66] S. Lee, H. H. J., and K. Y., “Modeling the role of TGF- β in regulation of the Th17 phenotype in the LPS-driven immune system,” *Bull. Math. Biol.*, vol. 76, pp. 1045–1080, 2014.

- [67] P. M. Ngina, R. W. Mbogo, and L. S. Luboobi, “Mathematical modelling of *in-vivo* dynamics of HIV subject to the influence of the CD8⁺ T-cells,” *Appl. Math.*, vol. 8, pp. 1153–1179, 2017.
- [68] M. J. Piotrowska, “An immune system-tumour interactions model with discrete time delay: Model analysis and validation,” *Commun. Nonlin. Sci. Numer. Simul.*, vol. 34, pp. 185–198, 2016.
- [69] X. Li and H. Levine, “Bistability of the cytokine-immune cell network in a cancer microenvironment,” *Converg. Sci. Phys. Oncol.*, vol. 3, p. 024002, 2017.
- [70] L. Anderson, S. Jang, and J.-L. Yu, “Qualitative behavior of systems of tumor-CD4⁺-cytokine interactions with treatments,” *Math. Meth. Appl. Sci.*, vol. 38, pp. 4330–4344, 2015.
- [71] S. Roy, K. Shrinivas, and B. Bagchi, “A stochastic chemical dynamic approach to correlate autoimmunity and optimal vitamin-D range,” *PloS ONE*, vol. 9, no. 6, p. e100635, 2014.
- [72] M. Baker, S. Denman-Johnson, B. S. Brook, I. Gaywood, and M. R. Owen, “Mathematical modelling of cytokine-mediated inflammation in rheumatoid arthritis,” *Math. Med. Biol.*, vol. 30, pp. 311–337, 2013.
- [73] N. Rapin, E. Mosekilde, and O. Lund, “Bistability in autoimmune diseases,” *Autoimmunity*, vol. 44, no. 4, pp. 256–260, 2011.
- [74] D. Wodarz and V. A. A. Jansen, “A dynamical perspective of CTL cross-priming and regulation: implications for cancer immunology,” *Immunol. Lett.*, vol. 86, no. 3, pp. 213–227, 2003.
- [75] M. A. Nowak and R. M. May, *Virus dynamics*. Oxford University Press, Oxford, 2000.
- [76] S. D. Wolf, B. N. Dittel, F. Hardardottir, and C. A. Janeway Jr., “Experimental autoimmune encephalomyelitis induction in genetically B cell-deficient mice,” *J. Exp. Med.*, vol. 184, no. 6, pp. 2271–2278, 1996.
- [77] H.-J. Wu, I. I. Ivanov, J. Darce, K. Hattori, T. Shima, Y. Umesaki, D. R. Littman, C. Benoist, and D. Mathis, “Gut-residing segmented filamentous bacteria drive autoimmune arthritis via T helper 17 cells,” *Immunity*, vol. 32, no. 6, pp. 815–827, 2010.
- [78] A. S. Perelson and P. W. Nelson, “Mathematical analysis of HIV-1 dynamics in vivo,” *SIAM Rev.*, vol. 41, no. 1, pp. 3–44, 1999.
- [79] A. K. Abbas, A. H. H. Lichtman, and S. Pillai, *Cellular and molecular immunology*. Elsevier Health Sciences, 8th ed., 2014.
- [80] P. S. Kim, P. P. Lee, and D. Levy, “Modeling regulation mechanisms in the immune system,” *J. Theor. Biol.*, vol. 246, no. 1, pp. 33–69, 2007.
- [81] S. Sakaguchi, N. Sakaguchi, M. Asano, M. Itoh, and M. Toda, “Immunologic self-tolerance maintained by activated T cells expressing IL-2 receptor α -chains (CD25). Breakdown of a single mechanism of self-tolerance causes various autoimmune diseases,” *J. Immunol.*, vol. 155, no. 3, pp. 1151–1164, 1995.
- [82] C. A. Janeway, P. Travers, M. Walport, and M. J. Shlomchik, *Immunobiology: the immune system in health and disease*. New York: Garland Science, 6th ed., 2005.

- [83] M. R. Walker, B. D. Carson, G. T. Nepom, S. F. Ziegler, and J. H. Buckner, “*De novo* generation of antigen-specific $CD4^+CD25^+$ regulatory T cells from human $CD4^+CD25^-$ cells,” *Proc. Natl. Acad. Sci. USA*, vol. 102, no. 11, pp. 4103–4108, 2005.
- [84] N. J. Burroughs, B. M. P. M. de Oliveira, and A. A. Pinto, “Regulatory T cell adjustment of quorum growth thresholds and the control of local immune responses,” *J. Theor. Biol.*, vol. 241, no. 1, pp. 134–141, 2006.
- [85] N. A. Danke, D. M. Koelle, C. Yee, S. Beheray, and W. W. Kwok, “Autoreactive T cells in healthy individuals,” *J. Immunol.*, vol. 172, no. 10, pp. 5967–5972, 2004.
- [86] I. Baltcheva, L. Codarri, G. Pantaleo, and J.-Y. Le Boudec, “Lifelong dynamics of human $CD4^+CD25^+$ regulatory T cells: Insights from *in vivo* data and mathematical modeling,” *J. Theor. Biol.*, vol. 266, no. 2, pp. 307–322, 2010.
- [87] A. M. Thornton and E. M. Shevach, “ $CD4^+CD25^+$ immunoregulatory T cells suppress polyclonal T cell activation *in vitro* by inhibiting interleukin 2 production,” *J. Exp. Med.*, vol. 188, no. 2, pp. 287–296, 1998.
- [88] E. M. Shevach, R. S. McHugh, C. A. Piccirillo, and A. M. Thornton, “Control of T-cell activation by $CD4^+CD25^+$ suppressor T cells,” *Immunol. Rev.*, vol. 182, no. 1, pp. 58–67, 2001.
- [89] P. Yu, R. K. Gregg, J. J. Bell, J. S. Ellis, R. Divekar, H.-H. Lee, R. Jain, H. Waldner, J. C. Hardaway, M. Collins, *et al.*, “Specific T regulatory cells display broad suppressive functions against experimental allergic encephalomyelitis upon activation with cognate antigen,” *J. Immunol.*, vol. 174, no. 11, pp. 6772–6780, 2005.
- [90] C. Tanchot, F. Vasseur, C. Pontoux, C. Garcia, and A. Sarukhan, “Immune regulation by self-reactive T cells is antigen specific,” *J. Immunol.*, vol. 172, no. 7, pp. 4285–4291, 2004.
- [91] Q. Tang, J. Y. Adams, A. J. Tooley, M. Bi, B. T. Fife, P. Serra, P. Santamaria, R. M. Locksley, M. F. Krummel, and J. A. Bluestone, “Visualizing regulatory T cell control of autoimmune responses in nonobese diabetic mice,” *Nat. Immunol.*, vol. 7, no. 1, p. 83, 2006.
- [92] J. Carneiro, K. Leon, Í. Caramalho, C. V van den Dool, R. Gardner, V. Oliveira, M.-L. Bergman, N. Sepúlveda, T. Paixão, J. Faro, *et al.*, “When three is not a crowd: a Crossregulation model of the dynamics and repertoire selection of regulatory $CD4^+$ T cells,” *Immunol. Rev.*, vol. 216, no. 1, pp. 48–68, 2007.
- [93] C. Baecher-Allan, V. Viglietta, and D. A. Hafler, “Inhibition of human $CD4^+CD25^{high}$ regulatory T cell function,” *J. Immunol.*, vol. 169, no. 11, pp. 6210–6217, 2002.
- [94] F. Fatehi, S. N. Kyrychko, A. Ross, Y. N. Kyrychko, and K. B. Blyuss, “Stochastic effects in autoimmune dynamics,” *Front. Physiol.*, vol. 9, p. 45, 2018.
- [95] F. Fatehi, Y. N. Kyrychko, and K. B. Blyuss, “Effects of viral and cytokine delays on dynamics of autoimmunity,” *Mathematics*, vol. 6, p. 66, 2018.
- [96] Y. A. Kuznetsov, *Elements of applied bifurcation theory*. Springer Verlag, 2nd ed., 1998.
- [97] A. Skapenko, J. Leipe, P. E. Lipsky, and H. Schulze-Koops, “The role of the T cell in autoimmune inflammation,” *Arthritis Res. Ther.*, vol. 7(Suppl 2), pp. S4–S14, 2005.

- [98] R. Antia, V. V. Ganusov, and R. Ahmed, “The role of models in understanding CD8⁺ T-cell memory,” *Nature Rev. Immunol.*, vol. 5, no. 2, pp. 101–111, 2005.
- [99] C. Li and J. C. Sprott, “Variable-boostable chaotic flows,” *Optik*, vol. 127, pp. 10389–10398, 2016.
- [100] C. Li, J. C. Sprott, and H. Xing, “Hypogenetic chaotic jerk flows,” *Phys. Lett. A*, vol. 380, pp. 1172–1177, 2016.
- [101] C. Li, X. Wang, and G. Chen, “Diagnosing multistability by offset boosting,” *Nonlin. Dyn.*, vol. 90, pp. 1335–1341, 2017.
- [102] C. Li, J. C. Sprott, and H. Xing, “Constructing chaotic systems with conditional symmetry,” *Nonlin. Dyn.*, vol. 90, pp. 1351–1358, 2017.